

Machine Learning for the ECG Diagnosis and Risk Stratification of Occlusion Myocardial Infarction at First Medical Contact

Results from ECG-SMART Observational Trial

By

Salah S. Al-Zaiti, PhD;^{1*} Christian Martin-Gill, MD, MPH;^{1,2} Jessica K. Zègre-Hemsey, PhD, RN;³ Zeineb Bouzid, MS, PhD(c);¹ Ziad Faramand, MD, MS;³ Mohammad O. Alrawashdeh, PhD;⁵ Richard E. Gregg, MS;⁶ Stephanie Helman, RN, PhD(c);¹ Nathan Riek, MS;¹ Karina Kraevsky-Phillips, RN, PhD(c);¹ Gilles Clermont, MD;^{1,7} Murat Akcakaya, PhD;¹ Susan M. Sereika, PhD;¹ Peter Van Dam, PhD;⁸ Stephen W. Smith, MD;⁹ Yochai Birnbaum, MD;¹⁰ Samir Saba, MD;^{1,2} Ervin Sejdic, PhD;¹¹ and Clifton W. Callaway, MD, PhD^{1,2}

From

(1) University of Pittsburgh, Pittsburgh, PA, USA; (2) University of Pittsburgh Medical Center (UPMC), Pittsburgh, PA, USA; (3) University of North Carolina – Chapel Hill, NC, USA; (4) Northeast Georgia Health System, GA, USA; (5) Harvard Medical School, Boston, MA, USA; (6) Philips Healthcare, Cambridge, MA, USA; (7) VA Healthcare System, Pittsburgh, PA, USA; (8) University Medical Center Utrecht, The Netherlands; (9) Hennepin Healthcare and University of Minnesota, Minneapolis, MN, USA; (10) Baylor College of Medicine, Houston, TX, USA; and (11) University of Toronto & [North York General Hospital](#), Toronto, Canada

Trial Registration: ClinicalTrials.gov Identifier: NCT04237688

Funding: National Institute of Health grants # R01HL137761 (SSA), UL1TR001857 (SSA), K23NR017896 (JZH), and KL2TR002490 (JZH)

Conflicts of Interest: none

* **Corresponding Author:** ssa33@pitt.edu

Abstract: 149 / 150

Word count: ~~34,836-097~~ / 4,000 (excluding abstract, methods, and references)

References: 60 / 60

Display items: 6 / 6

Extended data display items: ~~7-8~~ / 10

30 **ABSTRACT**

31 Patients with occlusion myocardial infarction (OMI) and no ST-elevation on presenting ECG are
32 increasing in numbers. These patients have a poor prognosis and would benefit from immediate
33 reperfusion therapy, but we currently have no accurate tools to identify them during initial triage. Herein,
34 we report the first observational cohort study to develop machine learning models for the ECG
35 diagnosis of OMI. Using 7,313 consecutive patients from multiple clinical sites, we derived and
36 externally validated an intelligent model that outperformed practicing clinicians and other widely used
37 commercial interpretation systems, significantly boosting both precision and sensitivity. Our derived
38 OMI risk score provided enhanced rule-in and rule-out accuracy relevant to routine care, and when
39 combined with the clinical judgment of trained emergency personnel, this score helped correctly
40 reclassify one in three patients with chest pain. ECG features driving our models were validated by
41 clinical experts, providing plausible mechanistic links to myocardial injury.

42 The ECG diagnosis of acute coronary syndrome (ACS) in patients with acute chest pain is a
43 longstanding challenge in clinical practice.¹⁻⁴ Guidelines primarily focus on ST-segment elevation (STE)
44 for discerning patients with ST-elevation myocardial infarction (STEMI) vs. other forms of ACS.⁵⁻⁸ A
45 biomarker-driven approach is recommended in the absence of STE on the presenting ECG. This
46 diagnostic paradigm has two important limitations. First, around 24%–35% of patients with non-STEMI
47 have total coronary occlusion, referred to as occlusion myocardial infarction (OMI), and require
48 emergent catheterization.⁹⁻¹³ This vulnerable group, in contrast to ~~acute myocardial infarction~~ ACS with
49 an open artery (~~non-OMI~~) (**Extended Data Fig. 1**), suffers from unnecessary diagnostic and treatment
50 delays that are associated with higher mortality.¹⁴⁻¹⁷ This excess risk can be mitigated with enhanced
51 diagnostic criteria. Although important ECG signatures of OMI are frequently described in the
52 literature,¹⁸⁻²¹ they are subtle, involve the entire QRST complex, and are spatial in nature (i.e., changes
53 diluted across multiple leads).²²⁻²⁴ Visual inspection of ECG images by clinical experts, thus, is
54 suboptimal and leads to a high degree of variability in ECG interpretation.²⁵⁻²⁷

55 The second limitation is that cardiac biomarkers, including conventional or high sensitivity
56 troponin (hs-cTn), cannot differentiate OMI until peak level is reached, which is too late to salvage
57 myocardium. Positive troponin results (>99th percentile limit) come with a high false positive rate, and
58 approximately one-third of patients remain in a biomarker-indeterminate “observation zone” even after
59 serial sampling.^{28,29} More importantly, ~25% of acute myocardial infarction cases have a negative initial
60 hs-cTn, which is observed in both the STEMI and OMI subgroups.³⁰ Consequently, 25%-30% of
61 patients with OMI are not treated in a timely fashion, and around 63% (IQR 38%-81%) of patients
62 evaluated for chest pain at the emergency department are admitted to the hospital because of an
63 inconclusive initial assessment.³¹ These diagnostic limitations have created a costly, inefficient clinical
64 practice paradigm where most patients with chest pain are over-monitored while some patients with
65 OMI have delayed diagnosis and treatment, potentially contributing to the 14%–22% excess risk of
66 mortality seen in the non-STE ACS group (NSTEMI-ACS).^{15,32,33}

67 In our prior work, we designed prototype algorithms for AI-enabled ECG analysis and
68 demonstrated the clinical feasibility of screening for ACS in the prehospital setting.^{34,35} Herein, we
69 describe the first multisite, prospective, observational cohort study to evaluate the diagnostic accuracy
70 of machine learning for the ECG diagnosis and risk stratification of OMI at first medical contact in an
71 observer-independent approach (**Extended Data Fig. 2**). Our intelligent models were derived and
72 externally validated on 7,313 patients with chest pain from multiple clinical sites in the United States.
73 The results demonstrate the superiority of machine learning in detecting subtle ischemic ECG changes
74 indicative of OMI, outperforming practicing clinicians and other widely used commercial ECG
75 interpretation software. Our derived OMI risk score provides superior-enhanced rule-in and rule-out
76 accuracy when compared to the HEART score, helping correctly reclassify one in three patients with
77 chest pain. We identified the most important ECG features driving our model's classifications and
78 identified plausible mechanistic links to myocardial injury.

79 80 **RESULTS**

81 ***Sample Characteristics***

82 After excluding patients with cardiac arrest, ventricular tachyarrhythmias, confirmed prehospital
83 STEMI, and duplicate ECGs, our derivation cohort included 4,026 consecutive patients with chest pain
84 (age 59±16 years, 47% females, 5.2% OMI). The two external validation cohorts together included
85 3,287 patients (age 60±15 years, 45% females, 6.4% OMI) (**Fig. 1** and **Table 1**). Most patients in the
86 derivation and validation cohorts were in normal sinus rhythm (>80%) and around 10% were in atrial
87 fibrillation. Around 3% of patients had left bundle branch block (LBBB) and ~10% had ECG-evidence of
88 left ventricular hypertrophy (LVH). The derivation and validation cohorts were comparable in terms of
89 age, sex, baseline clinical characteristics, and 30-day cardiovascular mortality. The validation cohort,
90 however, had more Black and Hispanic minorities and a slightly higher rate of ACS and OMI. ~~The~~

91 presence of OMI, defined as a culprit coronary artery with a TIMI flow grade of 0-1, was adjudicated
92 from charts by independent reviewers blinded to all ECG analyses. A TIMI flow grade of 2 with
93 significant coronary narrowing (>70%) and peak 4th-generation (not high sensitivity) troponin of 5-10
94 ng/mL was also indicative of OMI.

95 **Algorithm Derivation and Testing**

96 The positive class for model training was the presence of OMI, defined as a culprit coronary
97 artery with a TIMI flow grade of 0-1, as adjudicated from charts by independent reviewers blinded to all
98 ECG analyses. A TIMI flow grade of 2 with significant coronary narrowing (>70%) and peak 4th
99 generation (not high sensitivity) troponin of 5-10 ng/mL was also indicative of OMI. The negative class
100 for model training was the absence of OMI, which included all other non-ACS etiologies or those with
101 non-coronary occlusive ACS subtypes.

102 Input data for model training was based on prehospital 12-lead ECGs obtained at first medical
103 contact. We selected 73 morphological ECG features out of 554 temporal-spatial metrics using a hybrid
104 data-driven and domain expertise approach.¹⁸ Using these features, ten classifiers were trained to learn
105 ischemic patterns between ACS and non-ACS groups and to estimate the probability of OMI:
106 regularized logistic regression, linear discriminant analysis, support vector machine, Gaussian Naïve
107 Bayes, random forest, gradient boosting machine, extreme gradient boosting, stochastic gradient
108 descent logistic regression, k-nearest neighbors, and artificial neural networks. We chose these
109 classifiers ~~because they learn different mathematical representations in the data, in order to~~
110 ~~maximize~~ing the chance of finding the best ~~fitting modeling approach approach~~ for ~~learning the~~
111 ~~mathematical representation~~ relating complex ECG data to underlying physiology.

112 The random forest model achieved the best bias-variance tradeoff for training and internal
113 testing. We compared the random forest against the ECG interpretation of practicing clinicians and
114 against the performance of a commercial ECG interpretation system that is FDA-cleared for "Acute MI"
115 diagnosis. On the hold-out test set, the random forest model (AUROC 0.91 [95% CI 0.87-0.96])

116 outperformed both practicing clinicians (AUROC 0.79 [95% CI 0.73-0.76], $p < 0.001$) and the commercial
117 ECG system (AUROC 0.78 [95% CI 0.70-0.85], $p < 0.001$) (**Fig. 2A**).

118 Next, we used probability density plots for OMI(+) and OMI(-) classes to denote the optimal
119 separation margins for risk prediction. As recommended by guidelines,⁶ we defined a risk score to
120 identify patients at low risk (OMI score < 5), intermediate risk (OMI score 5-20), and high risk (OMI
121 score > 20), with these cutoffs yielding excellent separation between classes (Log-rank chi-square
122 133.04, $df = 2$, $p < 0.001$) (**Fig. 2B, left panel**). Our OMI score classified 74.4% of patients as low-risk and
123 4.6% as high-risk. Using the low-risk group in a rule-out strategy yielded a sensitivity of 0.91 and a
124 negative predictive value (NPV) of 0.993, with an overall missed event rate of 0.5%. Using high-risk
125 class for a rule-in strategy yielded a specificity of 0.976 and a positive predictive value (PPV) of 0.514,
126 with an overall false discovery rate of 2%. Finally, we compared this OMI score to the HEART score,
127 which uses patient history, ECG data, age, risk factors, and troponin values (**Fig. 2B, right panel**). Our
128 OMI score, which is based on ECG data alone, classified 66% more patients as low risk than the
129 HEART score with a comparable false negative rate $< 1\%$, and classified fewer patients as high-risk and
130 with much higher precision (51% vs. 33%). The OMI score also triaged 50% fewer patients as
131 intermediate risk and still got better discrimination for OMI detection (11.2% vs. 5.6%).

132 **Model Explainability**

133 We used Tree SHAP algorithms to generate an importance ranking that explains the output of the
134 random forest model based on SHAP values estimated for the top 25 features (**Fig. 3A**). The features
135 with the greatest impact on classification output included slight ST-depression in leads V1, V2, I, and
136 aVL; slight ST-elevation in leads III and V4-V6; loss of concave pattern in anterior leads; T wave
137 enlargement in II and aVF and T flattening or inversion in I and aVL; prolonged $T_{peak} - T_{end}$ interval; T axis
138 deviation; increased repolarization dispersion; and distorted directions of activation and recovery
139 patterns. Most of these ECG patterns can be mechanistically linked to cardiac ischemia, suggesting
140 their clinical value as plausible features for OMI detection.

141

142 To better visualize these global ECG patterns detected by our model, we created pooled
143 population median beats for the OMI(+) class (n=414 ECGs), and superimposed these median beats
144 on the pooled population median beats of patients with normal sinus rhythm and OMI(-) status (n=9,072
145 ECGs) (**Fig. 3B**). Findings from this figure agree with the patterns derived from the SHAP values
146 described above. Specifically, this figure illustrates that OMI is associated with ST-depression and T
147 flattening in V1-V2, I, and aVL; slight ST-elevation in the anterior leads with loss in concave pattern;
148 peaked T wave in inferior leads; $T_{\text{peak}}-T_{\text{end}}$ prolongation (seen in many leads); global repolarization
149 dispersion (seen as peaked T in some leads and flattening in others); T axis deviation (away from the
150 left ventricle), and distorted activation and recovery patterns (seen in the horizontal plane as loss of R
151 wave progression in precordial leads with increased T wave discordance). Due to prevalent multivessel
152 disease in this cohort, these OMI patterns remained relatively consistent regardless of culprit location.

153 Nevertheless, to examine local explainability of feature importance, we used force plots on
154 individual cases to identify the features that met the contribution threshold of the random forest model
155 on a given ECG. These force plots were also examined by study investigators to further corroborate on
156 the clinical validity of model predictions. **Extended Data Fig. 3** shows a selected example of a 12-lead
157 ECG with its corresponding force plot for the local features contribution.

Formatted: Font: Bold

158 **External Validation**

159 We tested the final lock-out model on 3,287 patients from two independent external clinical
160 sites. Machine learning engineers were blinded to outcome data from other sites, and the pre-populated
161 model predictions were independently evaluated by the clinical investigators. Our model generalized
162 well and maintained high classification performance (AUROC 0.873 [95% CI 0.85-0.90]), outperforming
163 the classification performance of the commercial ECG system (AUROC 0.75 [95% CI 0.71-0.79],
164 $p < 0.001$) and practicing clinicians (AUROC 0.80 [95% CI 0.77-0.83], $p < 0.001$) (**Fig. 4A**). Our OMI risk
165 score was a strong predictor of OMI, independent from, age, sex, and other coronary risk factors (OR

10.6 [95% CI 6.78-16.64] for high-risk class and OR 2.85 [95% CI 1.91-4.28] for intermediate-risk class) (Fig. 4B). This risk score triaged 69% of patients in the low-risk group at a false-negative rate of 1.3% and identified 5.1% of patients as high-risk at acceptable true positive rate >50%. The overall sensitivity, specificity, PPV, and NPV for the OMI rule-in and rule-out strategy were 0.86 (95% CI 0.81-0.91), 0.98 (95% CI 0.97-0.99), 0.54 (95% CI 0.46-0.62), and 0.99 (95% CI 0.98-0.99), respectively. This diagnostic accuracy remained relatively similar across subgroups based on age, sex, race, comorbidities, and baseline ECG findings, indicating the lack of aggregation bias (Fig. 4C). In comparison, the sensitivity, specificity, PPV, and NPV for ECG overread by practicing clinicians were 0.58, 0.93, 0.36, and 0.97, and for the commercial ECG system 0.79, 0.80, 0.22, and 0.98, respectively.

Next, we ~~used decision analysis to~~ evaluate the incremental gain of our derived risk score in reclassifying patients at first medical contact (Fig. 5). ~~To simulate initial assessment by emergency personnel, we used~~ was based on the modified HEAR score (History, ECG, Age, and Risk factors) to triage patients into low, intermediate, and high-risk groups.³⁶ At baseline, emergency personnel triaged 48% of patients as low risk with a NPV of 99.0% and triaged 3% of patients as high risk with a PPV of 54.1%. Nearly 50% of patients remained in an indeterminate observation zone. Applying our OMI risk score would help triage 45% more patients as low risk while keeping the NPV at 98.8% and would help detect 85% more cases with OMI while keeping PPV at 50.0%. The OMI score would also help reduce the number of patients in the indeterminate observation zone by more than half. These numbers translate into a net reclassification improvement (NRI) index of 41% (95% CI 33%-50%). To validate this incremental clinical utility, we manually reviewed ECGs reclassified correctly as OMI(+) (Extended data Fig. 34). Many of these ECGs showed subtle or nonspecific changes that were nondiagnostic as per guidelines,⁵ suggesting potential value in boosting provider's confidence when interpreting "fuzzy" ECGs.

Finally, we investigated the potential sources of false negatives in the validation data. Among those with missed OMI events (n=28, 0.9%), many patients had high-frequency noise and baseline

191 wander on their initial ECG (n=13/28, 46%) or had low voltage ECG (n=14/28, 50%), and most patients
192 (n=24/28, 86%) had benign ECGs without any diagnostic ST-T changes (**Extended Data Fig. 45**).
193 Moreover, we found no significant differences between false negatives and true positives in terms of
194 demographics or clinical characteristics, with the exception that most false negatives had a history of a
195 prior myocardial infarction (93% vs. 27%). The latter finding was intriguing given that our OMI model
196 was slightly less specific in patients with known coronary artery disease (**Fig. 4C**). This finding aligns
197 with recent evidence showing diminished NPV in patients with chest pain and known CAD.³⁷

198 **Screening for Any ACS Event**

199 We further built a model to screen for any potential ACS event at first medical contact. Using the
200 same set of ECG features, we trained and optimized a random forest classifier that denotes the
201 likelihood of any ACS event. The model performed well during training (AUROC 0.88 [95% CI 0.87-
202 0.90]) and generalized well during internal testing (AUROC 0.80 [95% CI 0.76-0.84]), outperforming
203 both the commercial ECG interpretation system (AUROC 0.62 [95% CI 0.55-0.68], p<0.001) and
204 practicing clinicians (AUROC 0.66 [95% CI 0.59-0.72], p<0.001) (**Extended Data Fig. 56**). On external
205 validation, the model continued to generalize well (AUROC 0.79 [95% CI 0.76-0.81]), outperforming the
206 commercial system (AUROC 0.68 [95% CI 0.65-0.71], p < 0.001) and practicing clinicians (AUROC
207 0.72 [95% CI 0.69-0.74], p < 0.001). Our derived risk score provided a suboptimal rule-out classification
208 for any ACS event (sensitivity 68.2% and NPV 92.5%) but provided superior rule-in accuracy
209 (specificity 98.9% and PPV 82.5%).

210 **DISCUSSION**

211 In this study, we developed and validated a machine learning algorithm for the ECG diagnosis
212 of OMI in consecutive patients with chest pain recruited from multiple clinical sites in the United States.
213 This model outperformed practicing clinicians and other commercial interpretation systems. The derived
214 risk score provided superior rule-in and rule-out accuracy for OMI, boosting the sensitivity by 7 to 28
215 percentage points and the precision by 18 to 32 percentage points compared to reference standards.

216 When combined with the judgment of experienced emergency personnel, our derived OMI risk score
217 helped correctly reclassify one in three patients with chest pain. To our knowledge, this is the first study
218 using machine learning methods and novel ECG features to optimize OMI detection in patients with
219 acute chest pain and negative STEMI pattern on their baseline ECG at first medical contact.

220 Mapping myocardial ischemia, a problem of regional metabolic derangement, to coronary
221 occlusion, a problem of diminished blood flow due to an atherosclerotic plaque rupture, is a complex
222 process.¹ Essentially, ischemia disproportionately distorts action potentials in different myocardial
223 segments, resulting in tissue-scale currents, often called 'injury' currents. Prior studies have mapped
224 significant ST-elevation to transmural injury currents associated with total coronary occlusion. This has
225 historically driven the current paradigm dichotomy of STEMI vs. 'others' (any ACS other than STEMI) in
226 determining who might benefit from emergent reperfusion therapy. However, nearly 65% of patients
227 with ACS present with no ST-elevation on their baseline ECG,^{35,38} and among the latter group,
228 24%–35% have total coronary occlusion requiring emergent catheterization.⁹⁻¹³ Thus, determining who
229 would benefit from reperfusion therapy remains an adjudicated diagnosis.

230 Conceptually, injury currents produced by ischemic cardiac cells are summative in nature,
231 explaining how ST amplitude changes can get attenuated on the surface ECG (**Extended Data Fig.**
232 **67**). These injury currents, however, distort the propagation of both excitation and recovery pathways,
233 altering the configuration of the QRS complex and the STT waveform altogether.³⁹ Thus, a more
234 comprehensive approach for the ECG detection of ischemia should focus on (1) evaluating temporal
235 characteristics over entire waveform segments rather than the voltage at a given time point (e.g., J+80),
236 and (2) evaluating lead-to-lead spatial characteristics in waveform morphology rather than absolute
237 changes in isolated ECG leads.¹

238 This study has identified several ECG patterns indicative of acute coronary occlusion beyond
239 the criteria recommended by clinical guidelines.⁵ Intriguingly, these ECG patterns overlap with those
240 described in the literature. A consensus report in 2012 identified few ECG patterns that should be

241 treated as STEMI equivalent during acute pain episodes: ST-depression in V1 to V3; small inverted T
242 waves in V1 to V3; deep negative T waves in precordial leads; widespread ST-depression, and
243 prominent positive T waves.²⁰ Similar ECG patterns were also described more recently: ST-depression
244 in V1 to V4 (versus V5-V6); reciprocal ST-depression with maximal ST-depression vector towards the
245 apex (leads II and V5, with reciprocal STE in aVR); subtle ST-elevation; acute pathologic Q waves;
246 hyperacute T waves; and loss of terminal S wave.²¹ Many of these expert-driven patterns rely on
247 assessing the proportion of repolarization amplitudes or area under the QRS amplitude. They also rely
248 heavily on the visual assessment of waveform morphology and can introduce a high degree of
249 subjectivity and variability among ECG interpreters. We demonstrated that the machine learning
250 models described herein not only outperform practicing clinicians in identifying OMI, but also provided
251 an objective, observer-independent approach to quantify subtle ECG patterns associated with OMI.

252 Many of the data-driven features identified by our machine learning model are subtle and cannot
253 be easily appreciated by clinical experts. T feature indices were among these most important features,
254 including $T_{\text{peak}}-T_{\text{end}}$ interval prolongation, T wave flattening, and T wave characteristics at the inflection
255 point preceding T_{peak} (**Fig. 3A**). Mechanistically, ischemic injury currents interfere with signal
256 propagation leading to longer activation time.⁴⁰ These late activation potentials lead to a loss of terminal
257 S wave and longer recovery time, both manifesting as T wave flattening, shifted T peak, and loss of
258 concavity at the initial T wave (**Fig. 3B**). These STEMI-equivalent patterns were previously described in
259 the literature as small or negative T waves with widespread ST-depression or subtle ST- elevation.^{20,21}
260 Another important subtle feature identified by our model was increased ventricular repolarization
261 dispersion, measured using the ratio between the principal components of the STT waveforms (i.e.,
262 PCA metrics), the direction of the T axis, and the angle between activation and recovery pathways
263 (e.g., total-cosine-R-to-T). Injury currents disproportionately affect the duration and velocity of
264 repolarization across different myocardial segments,⁴¹ resulting in lead-to-lead variability in the
265 morphology of the STT waveform.^{22-24,39,42} These high-risk ECG patterns were previously described as
266 a mixture of deep negative T waves and prominent / hyperacute T waves or reciprocal T wave

267 changes.^{20,21} Despite their subtle nature, our machine learning model provided a more comprehensive,
268 quantitative approach to evaluating this inter-lead variability in repolarization morphology.

269 Machine learning is well-suited to address many challenges in 12-lead ECG interpretation.
270 Myocardial ischemia distorts the duration and amplitude of the Q wave, R peak, R', QRS complex, ST
271 segment, and T wave, as well as the morphology and configuration of these waveforms (e.g.,
272 upsloping, down-sloping, concavity, symmetry, notching, etc.). These distortions are lead-specific yet
273 come with dynamic inter-lead correlations. Thus, ECG interpretation involves many complex aspects
274 and parameters, making it a highly dimensional, decision space problem.¹ Few experienced clinicians
275 excel in such pattern recognition,²¹ which explains why so many OMI cases are not reperused in a
276 timely way; this is also why simple, rule-based commercial systems that use simple regression models
277 are suboptimal for OMI detection. Machine learning algorithms can provide powerful tools to solve such
278 highly dimensional, non-linear mathematical representations found in 12-lead ECG data.

279 Although the literature on machine learning for the ECG diagnosis of coronary disease is
280 ubiquitous, it comes with many serious limitations. First, many studies focused on detecting the known
281 STEMI group or other subtle ACS phenotypes^{34,35,43,44} rather than the critical group without ST-
282 elevation, which is not classified as STEMI and is therefore excluded from STEMI databases. Second,
283 most prior work used open-source ECG datasets like PTB and PTB-XL,⁴⁵ which are highly selected
284 datasets that focus on ECG-adjudicated diagnoses. Our unique cohorts included unselected,
285 consecutive patients with clinical profiles and disease prevalence like that seen in real-world settings.
286 Third, many studies used a full range of input features based on both ECG data and clinical data
287 elements (e.g., patient history, physical exam abnormalities, laboratory values, diagnostic tests),⁴⁶⁻⁴⁹
288 which limits the applicability to real-world settings. Fourth, to our knowledge, most studies used a single
289 derivation cohort for training and testing,⁵⁰ without the use of an independent validation cohort. Finally,
290 prior studies paid little attention to model explainability,⁵¹ shedding little light on novel markers and

291 pathways of ischemia than what is already known. Without explanation aids of clinical meaningfulness,
292 machine learning models for ECG interpretation would have limited clinical utility.⁵²

293 This study has important clinical implications. Our machine learning model can be integrated
294 into systems of care for real-time deployment where risk score assignments can be made readily
295 available to clinicians right at time of ECG acquisition. Such enhanced decision support can help
296 emergency personnel identify 85% more patients with critical coronary occlusion despite the absence of
297 a STEMI pattern on the presenting ECG and without any loss in precision. Our models can also help
298 inform care in more than 50% of patients in whom the initial assessment is indeterminate, placing 45%
299 more patients in the low-risk group for OMI without any loss in NPV. This incremental gain in rule-in and
300 rule-out accuracy can help re-allocate critical emergency resources to those in utmost need while
301 optimizing the clinical workflow. This can impact numerous decisions at first medical contact, including
302 targeted prehospital interventions, catheterization lab activation, administration of anti-ischemic
303 therapies, hospital destination decisions, the need for medical consults, referrals for expedited
304 diagnostic testing (e.g., echocardiogram, imaging scans), and early discharge decisions. Furthermore,
305 until now, clinicians never had sensitive nor highly specific tools that would allow the ultra-early
306 identification of OMI in the absence of a STEMI pattern. Such enhanced diagnostics can allow the
307 design and implementation of prospective interventional trials to assess the therapeutic effectiveness of
308 targeted interventions in this vulnerable group (e.g., early upstream P2Y₁₂ inhibitor administration,⁵³
309 emergent vs. delayed reperfusion therapy,⁵⁴ glucose-insulin-potassium infusion,⁵⁵ etc.).

310 Several limitations merit consideration. First, the engineered features we used for building our
311 models are based on a manufacturer-specific software. There are known discrepancies between
312 manufacturers in ECG preprocessing and metrics computation, which means that our models would
313 need retraining and validation when using different software for ECG signal processing. Alternatively,
314 deep neural networks can be used to directly analyze raw ECG signal without explicit feature
315 engineering. However, these techniques require much larger sample size for model derivation (e.g.,

316 >10,000) and might not yield a meaningful improvement over feature engineering-based machine
317 learning approaches for traditional 12-lead ECG based diagnosis.⁵⁶ Second, we found slight differences
318 between the derivation and validation cohorts, specifically in terms of disease prevalence and practicing
319 clinicians' accuracy in ECG interpretation. These cohorts came from two different regions in the U.S.,
320 and EMS systems follow state-specific protocols. It is possible that discrepancies in EMS protocols and
321 in-hospital practices resulted in slight differences in the types and proportions of patients that receive
322 prehospital 12-lead ECGs, as well as in their outcome adjudications. Yet, it is reassuring that our
323 models continued to generalize well between the study sites. Third, it is worth noting that our model for
324 screening for "any ACS event" only boosted the performance of the rule-in arm of the derived risk
325 score. This means that a low-risk determination by our model suggests that a given patient would
326 unlikely have OMI, but they might still have a less subtle phenotype of NSTEMI-ACS that does not require
327 reperfusion therapy. It is likely that serial ECG testing might improve the detection of this group missed
328 events where a patients might switch to a higher risk category in the following hours,³⁴ but this remains
329 to be confirmed. Coronary occlusion is a dynamic process that evolves over time, so an initial low risk
330 class by our models should not lead to a lower level of active monitoring. Finally, although this study
331 used prospective patients, all analyses were completed asynchronously with patient care. Prospective
332 validation where OMI probabilities and decision support is provided in real time is warranted.

333 In conclusion, we developed and externally validated machine learning models for the ECG
334 diagnosis of OMI in 7,313 patients with chest pain from multiple sites in the United States. The results
335 demonstrated the superiority of machine learning in detecting subtle ischemic ECG changes indicative
336 of OMI in an observer-independent approach. These models outperformed practicing clinicians and
337 commercial ECG interpretation software, significantly boosting both precision and recall. Our derived
338 OMI risk score provided superior-enhanced rule-in and rule-out accuracy when compared to HEAR
339 score, and when combined with the clinical judgment of trained emergency personnel, this score helped
340 correctly reclassify one in three patients with chest pain. The ECG features driving our models were

341 evaluated, providing plausible mechanistic links to myocardial injury. Future work should focus on the
342 prospective validation where OMI probabilities and decision support is provided in real time.

343 **ACKNOWLEDGMENTS**

344 This study was funded by grants from the National Institute of Health (NIH), National Heart, Lung, and Blood
345 Institute (NHLBI), National Center for Advancing Translational Sciences (NCATS), and National Institute for
346 Nursing Research (NINR) through grants # R01HL137761 (SSA), UL1TR001857 (SSA), K23NR017896 (JZH),
347 and KL2TR002490 (JZH).

348 **AUTHOR CONTRIBUTION**

349 SSA, CMG, JZH, SS, ES, and CWC conceived the study, secured funding, and supervised the research. YB and
350 SWS advised on the scientific direction of the study. SSA, JZH, ZF, MOA, KKP, and SH supervised dataset
351 creation and annotation. SSA, CMG, JZH, ZF, MOA, and SH supervised clinical outcomes adjudication. REG,
352 SSA, MA, ZB, PVD, and NR supervised ECG signal processing and feature extraction. SSA, ZB, NR, SMS, and
353 ES performed feature engineering, machine learning modeling, statistical analysis, and results interpretation. SSA
354 drafted the manuscript. All authors critically revised the manuscript for important intellectual content. All authors
355 provided their final approval of the version to be published. All authors are accountable for the work.

356 **DECLARATION OF INTERESTS**

357 US Patent # 10820822, Owner: University of Pittsburgh, Inventors: SSA, ES, and CWC.

358 **DATA AVAILABILITY**

359 The ECG SMART trial makes use of extracted ECG features to train and evaluate a random forest classifier to
360 denote the probability of OMI. The Python codes to evaluate these models along with the derivation and external
361 validation datasets are available through GitHub ([https://github.com/zeineb-bouzid/sharing-github-nature-](https://github.com/zeineb-bouzid/sharing-github-nature-medicine.git)
362 [medicine.git](https://github.com/zeineb-bouzid/sharing-github-nature-medicine.git)). Researchers wishing the source binary files to design alternative models should contact the
363 corresponding author to arrange for proper approvals and institutional data use agreements.

364 **CODE AVAILABILITY**

365 The Python codes to evaluate these models along with the derivation and external validation datasets are
366 available through GitHub (<https://github.com/zeineb-bouzid/sharing-github-nature-medicine.git>).

367

368 **ONLINE METHODS**

369 **Ethics Statement**

370 The derivation cohort included prehospital data from the City of Pittsburgh Bureau of
371 Emergency Medical Services (EMS) and in-hospital data from three tertiary care hospitals from the
372 University of Pittsburgh Medical Center (UPMC) healthcare system: UPMC Presbyterian Hospital,
373 UPMC Shadyside Hospital, and UPMC Mercy Hospital (Pittsburgh, Pennsylvania, USA). All
374 consecutive eligible patients were recruited under a waiver of informed consent. This observational trial
375 was approved by the institutional review board of the University of Pittsburgh and was registered in
376 www.ClinicalTrials.gov (identifier # NCT04237688). The analyses described in this paper were
377 prespecified by the trial protocol that was funded by the National Institute of Health. The first external
378 validation cohort included data from Orange County EMS (Chapel Hill, North Carolina, USA). This study
379 actively consented eligible patients and was approved by the institutional review board of the University
380 of North Carolina at Chapel Hill. The second external validation cohort included data from Mecklenburg
381 County EMS and Atrium Health (Charlotte, North Carolina, USA). Data were collected through a
382 healthcare registry and all consecutive eligible patients were enrolled under a waiver of informed
383 consent. This study was also approved by the institutional review board of the University of North
384 Carolina at Chapel Hill. These two external cohorts were very comparable and were, therefore,
385 combined into one cohort.

386 **Study Design & Data Collection**

387 This was a prospective, observational cohort study. The methods for each study cohort were
388 described in detail elsewhere.^{57,58} All study cohorts enrolled adult patients with an emergency call for
389 non-traumatic chest pain or anginal equivalent symptoms (arm, shoulder, jaw pain, shortness of breath,
390 diaphoresis, syncope). Eligible patients were transported by an ambulance and had at least one
391 recorded prehospital 12-lead ECG. There were no selective exclusion criteria based on sex, race,

392 comorbidities, or acuity of illness. For this prespecified analysis, we only included non-duplicate ECGs
393 from unique patient encounters, and we removed patients with prehospital ECGs showing ventricular
394 tachycardia or ventricular fibrillation (i.e., these patients are managed by ACLS algorithms). We also
395 removed patients with confirmed prehospital STEMI, which included machine-generated ***ACUTE
396 MI*** warning, EMS-documentation of STEMI, and medical consult for potential CATH lab activation.

397 Independent reviewers extracted data elements from hospital systems on all patients meeting
398 eligibility criteria. If a prehospital ECG had no patient identifiers, we used a probabilistic matching
399 approach to link each encounter with the correct hospital record. This previously validated data linkage
400 protocol was based on the ECG-stamped birth date, sex, and date/time logs, as well as based on EMS
401 dispatch logs and receiving hospital records. All probabilistic matches were manually reviewed by
402 research specialists for accuracy. The match success rate ranged from 98.6% to 99.8%.

403 **Clinical Outcomes**

404 Adjudications were made by independent reviewers at each local site after reviewing all
405 available medical records within 30 days of the indexed encounter. Reviewers were blinded from all
406 ECG analyses and models' predictions. OMI was defined as coronary angiographic evidence of an
407 acute culprit lesion in at least one of the three main coronary arteries (LAD, LCX, RCA) or their primary
408 branches with TIMI flow grade of 0-1. TIMI flow grade of 2 with significant coronary narrowing > 70%
409 and peak troponin of 5-10.0 ng/mL was also considered indicative of OMI.^{17,21} These adjudications
410 were made by two independent reviewers. The Kappa coefficient statistic between the two reviewers
411 was 0.771 (i.e., substantial agreement). All disagreements were resolved by a third reviewer.

412 ACS was defined per the fourth universal definition of myocardial infarction as the presence of
413 symptoms of ischemia (i.e. diffuse discomfort in the chest, upper extremity, jaw, or epigastric area for
414 more than 20 minutes) and at least one of the following criteria: (1) subsequent development of labile,
415 ischemic ECG changes (e.g., ST changes, T inversion) during hospitalization; (2) elevation of cardiac
416 troponin (i.e., > 99th percentile) during the hospital stay with rise and/or drop on serial testing; (3)

417 coronary angiography demonstrating greater than 70% stenosis, with or without treatment; and/or (4)
418 functional cardiac evaluation (stress testing) that demonstrates ECG, echocardiographic, or
419 radionuclide evidence of focal cardiac ischemia.⁵ Patients with type 2 MI and pre-existing subacute
420 coronary occlusion were labeled as negative for ACS and OMI. This included around 10% of patients
421 with positive troponin but with no rise and/or drop in concentration on serial testing (i.e., chronic leak) or
422 with troponin leak attributed to non-coronary occlusive conditions such as pericarditis. On a randomly
423 selected small subset of patients (n=1,209), the Kappa coefficient statistic for ACS adjudication ranged
424 from 0.846 to 0.916 (i.e., substantial to perfect agreement).

425 **ECG Methods**

426 Prehospital ECGs were obtained in the field by paramedics as part of routine care. ECGs were
427 acquired using either Heart Start MRX (Philips Healthcare) or LIFEPAK-15 (Physio-Control Inc.)
428 monitor-defibrillator devices. All digital 12-lead ECGs were acquired at a sampling rate of 500 s/s (0.05-
429 150 Hz) and transmitted to the respective EMS agency and receiving hospital. Digital ECG files were
430 exported in XML format and stored in a secondary server at each local site. ECG images were de-
431 identified and manually annotated by independent reviewers or research specialists; ECGs with poor
432 quality or missing leads were removed from the study. Next, digital XML files were transmitted to the
433 Philips Advanced Algorithm Research Center for offline analysis (Cambridge, Massachusetts, USA).

434 ECG featurization was described in detail elsewhere.¹⁸ Briefly, ECG signal preprocessing and
435 feature extraction were performed using a manufacturer-specific software (Philips DXL diagnostic 12/16
436 lead ECG analysis program). ECG signals were first preprocessed to remove noise, artifacts, and
437 baseline wander. Ectopic beats were removed, and median beats were calculated for each lead. Next,
438 we used the root mean square (RMS) signal to identify global waveform fiducials, including the onset,
439 offset, and peak of the P wave, QRS complex, and T wave. Lead-specific fiducials were then identified
440 to further segment individual waveforms into Q, R, R', S, S', and J point.

441 We then computed a total of 554 ECG features based on (1) the amplitude, duration, area,
442 slope and/or concavity of global and lead-specific waveforms; (2) the QRS and T axes and angles in
443 the frontal, horizontal, spatial, XY, XZ, and YZ planes, including directions at peak, inflection point, and
444 initial / terminal loops; (3) eigenvalues of the principal components of orthogonal ECG leads (I, II, V1-
445 V6), including PCA ratios for individual ECG waveform segments; and (4) T loop morphology
446 descriptors. Features with zero distribution were removed to prevent representation bias.

447 Next, we previously identified an optimal parsimonious list of the most important ECG features
448 that are mechanistically linked to cardiac ischemia as described in detail elsewhere.¹⁸ Briefly, to prevent
449 omitted-feature bias, we used a hybrid approach that combines domain knowledge with a data-driven
450 strategy. First, clinical scientists identified 24 classical features that are known to correlate with cardiac
451 ischemia (i.e., lead-specific ST-80 and T wave amplitudes). Next, starting with a comprehensive list of
452 554 candidate features, we used data-driven algorithms (e.g., recursive feature elimination and
453 LASSO) to identify 198 supplemental features potentially related to ischemia. LASSO selects features
454 with non-zero coefficients after L1 norm regularization, and recursive feature elimination uses repeated
455 regression iterations to identify the features that have significant impact on model predictions. We then
456 examined the feature pairs in this expanded list of 222 features and removed features with very high
457 collinearity scores that contains redundant information (e.g., we kept QTc if both QT and QTc were
458 selected by the model). Finally, we used feature importance ranking to identify the most parsimonious
459 subset of features that are complementary and can boost the classification performance. This hybrid
460 approach eventually yielded a subset of 73 features that can serve as plausible markers of
461 ischemia~~Clinical scientists initially reviewed a list of 554 features and marked the ones that are known~~
462 ~~to correlate with cardiac ischemia. This list was then expanded by supplemental features identified by~~
463 ~~data driven algorithms (e.g., recursive feature elimination and LASSO). The clinical scientists then~~
464 ~~reviewed the expanded list to examine feature pairs with high collinearity and retained the subset of~~

465 ~~features that are complementary and can serve as plausible markers of ischemia. This approach~~
466 ~~eventually yielded a subset of 73 features that was shown to boost classification performance.~~¹⁸

467 **Machine Learning Methods**

468 We followed best practices recommended by “ROBUST-ML” and “ECG-AI stress test” checklists
469 to design and benchmark our machine learning algorithms.^{51,59} To prevent measurement bias, ECG
470 features were manually reviewed to identify erroneous calculations. Physiologically plausible outliers
471 were replaced with ± 3 SD. On average, each feature had a 0.34% missingness rate (range 0.1% to
472 1.6%). Thus, we imputed missing values with the mean, median, or mode of that feature after
473 consultation with clinical experts. ECG metrics were then z-score normalized and used as input
474 features in machine learning models. The derivation and validation datasets were cleaned
475 independently to prevent data leakage. Both cohorts were recruited over the same time window,
476 suggesting the lack of temporal bias. To prevent potential mismatch with intended use, input features
477 for model development included only ECG data plus the machine-stamped age. No other clinical data
478 were used for model building.

479 We randomly split the derivation cohort into an 80% training set and a 20% internal testing set.
480 On the training set, we fit 10 machine learning classifiers: regularized logistic regression, linear
481 discriminant analysis, support vector machine, Gaussian Naïve Bayes, random forest, gradient
482 boosting machine, extreme gradient boosting, stochastic gradient descent logistic regression, k-nearest
483 neighbors, and artificial neural networks. Each classifier was optimized over 10-fold cross validation to
484 finetune hyperparameters. After selecting optimal hyperparameters, models were re-trained on the
485 entire training subset to derive final weights and create a lockout model to evaluate on the holdout test
486 set. We calibrated our classifiers to produce a probabilistic output which can be interpreted as a
487 confidence level (probability risk score). Trained models were compared using the AUROC curve with
488 Wilcoxon signed-rank test for pairwise comparisons. ROC-optimized cutoffs were chosen using Youden
489 index, and classifications on confusion matrix were compared using McNemar's test.

490 The random forest classifier (RF) achieved high accuracy on the training set (low bias) with a
491 relatively small drop in performance on the test set (low variance), indicating an acceptable bias-
492 variance tradeoff and low risk of overfitting (**Extended Data Fig. 78**). Although the support vector
493 machine (SVM) model had lower variance on the test set, when compared with the RF model, there
494 were no significant differences in AUROC (DeLong's test) or their binary classifications (McNemar's
495 test). Moreover, there were no differences between the RF and SVM models in terms of Kolmogorov-
496 Smirnov goodness-of-fit (0.716 vs. 0.715) or the Gini purity index (0.82 vs. 0.85). Due to its scalability
497 and intuitive architecture, we chose the probability output of the RF model to build our derived OMI
498 score. We generated density plots of these probability scores for positive and negative classes and
499 selected classification thresholds for low, intermediate, and high-risk groups based on prespecified
500 NPV > 0.99 and TPR > 0.50. Finally, we used the lock-out random forest classifier to generate
501 probability scores and risk classes on the completely unseen external validation cohort. The code to
502 generate probability scores is included with the supplemental materials of this manuscript.

503 **Reference Standard**

504 To reduce the risk of evaluation bias, we benchmarked our machine learning models against
505 multiple reference standards used during routine care in clinical practice. First, we used a commercial,
506 FDA-approved, ECG interpretation software (Philips DXL diagnostic algorithm) to denote the likelihood
507 of ischemic myocardial injury. This likelihood (yes/no) was based on a composite of the followings: (1)
508 diagnostic codes for ">>>Acute MI<<<", including descriptive statements that denote "acute", "recent",
509 "age indeterminate", "possible" or "probable"; and (2) diagnostic codes for ">>>Acute Ischemia<<<",
510 including descriptive statements that denote "possible", "probable", or "consider". Diagnostic statements
511 that denoted "old" [infarct], "nonspecific" [ST depression], or "secondary to" [LVH or high heart rate]
512 were excluded from this composite reference standard.

513 We also used practicing clinicians' overread of ECGs to denote the likelihood of ischemic
514 myocardial injury on a given ECG (yes/no) when a STEMI pattern does not exist, which is congruent

515 with how ED physicians evaluate these patients in clinical practice. Independent physician reviewers
516 annotated each 12-lead ECG image as per the fourth universal definition of MI criteria,⁵ including two
517 contiguous leads with ST-elevation (≥ 0.2 mV for V2-V3 in men ≥ 40 years and ≥ 2.5 mm in men < 40
518 years; ≥ 0.15 mV for V2-V3 in women; or ≥ 0.1 mV in other leads) or ST-depression (new horizontal or
519 down-sloping depression ≥ 0.05 mV); with or without T wave inversion (> 0.1 mV in leads with
520 prominent R wave or R/S ratio > 1). Reviewers were also prompted to use their clinical judgment to
521 identify highly suspicious ischemic changes (e.g., reciprocal changes, hyperacute T waves), as well as
522 to account for potential confounders (e.g., bundle branch blocks, early repolarization). On a randomly
523 selected subset of patients in the derivation cohort (n=1,646), the Kappa coefficient statistic between
524 two emergency physicians who interpreted the ECGs was 0.568 (i.e., moderate agreement). A third
525 reviewer was used to adjudicate discrepancies on this randomly selected subset. Similarly, on a
526 randomly selected subset of patients in the external validation cohort (n=375), the Kappa coefficient
527 statistic between the two board-certified cardiologists who interpreted the ECGs was 0.690 (i.e.,
528 substantial agreement).

529 Finally, given that clinicians largely depend on risk scores to triage patients in the absence of STEMI,
530 which would significantly affect how OMI patients are diagnosed and treated in clinical practice, we
531 compared our derived OMI risk score against the HEART ~~risk~~-score. This score is commonly used in
532 US hospitals and it has been well-validated for triaging patients in the emergency department.⁶⁰ The
533 HEART score is based on the patient's History at presentation, ECG interpretation, Age, Risk factors,
534 and initial Troponin values (range 0-10). This score places patients in low (0-3), intermediate (4-6), and
535 high-risk (7-10) groups. Given that troponin results are not usually available at first medical contact, we
536 used a modified HEAR score after dropping the Troponin values, which has also been previously
537 validated for use by paramedics prior to hospital arrival.³⁶ The comparison against the HEART score
538 herein focused on establishing the incremental gain of using the derived OMI score over routine care at
539 initial triage. We compared how the new risk classes assigned by our derived OMI score

540 agree with or differ from the risk classes assigned by the HEART score, which could inform
541 potential incremental gain over routine care.

542 **Statistical Analysis**

543 Descriptive statistics were reported as mean \pm standard deviation or n (%). Missing data was
544 assessed for randomness and was handled during ECG feature selection (see Machine Learning
545 Methods section above). Normality of distribution was assessed prior to hypothesis testing where
546 deemed necessary. ECG features were z-score normalized as part of standard input architectures for
547 machine learning models. Comparisons between cohorts were performed using chi-square (for discrete
548 variables) and independent samples t-test or Mann-Whitney U test (for continuous variables). The level
549 of significance was set at alpha 0.05 for two-tailed hypothesis testing where applicable.

550 All diagnostic accuracy values were reported as per STARD recommendations (Reporting
551 Guidelines for Diagnostic Accuracy Studies). We reported classification performance using AUROC
552 curve, sensitivity (recall), specificity, PPV (precision), and NPV, along with 95% confidence interval (CI)
553 where applicable. For 10-fold cross validation, we compared the multiple classifiers using the Wilcoxon
554 signed-rank test (for AUROC curves) and McNemar's test (for confusion matrices). We derived low-,
555 intermediate-, and high-risk categories for the final classifier using Kernel density plot estimates
556 between classes. The adequacy of these risk classes was evaluated using Log-rank chi-square of
557 accumulative risk for clinically important outcomes over the length of stay during the indexed
558 admission.

559 For assessing the incremental gain in classification performance, we compared the AUROC of
560 the final model against reference standards using DeLong's test. For ease of comparison, the
561 confidence bounds for AUROC of the reference standards (commercial system and practicing
562 clinicians) were generated using 1000 bootstrap samples. To place the incremental gain value in a
563 broader context of the clinical workflow, We-we then-also computed the Net Reclassification
564 Improvement (NRI) index of our model against the HEAR score during the initial assessment at first

565 medical contact. Risk scores are an integral part of clinical workflow in patients with suspected ACS
566 who do not meet STEMI criteria. As per STARD recommendations (Reporting Guidelines for Diagnostic
567 Accuracy Studies), the NRI Index evaluates the net gain between up-triage and down-triage when
568 correctly reclassifying risk class assignments of an “old” test (HEART score) using a “new” test (the
569 derived OMI score).

570 We used logistic regression to identify the independent predictive value of OMI risk classes. We
571 used variables significant in univariate analysis and then built multivariate models with stepwise
572 backward selection method using Wald chi-square criteria. We reported odds ratios with 95% CI for all
573 significant predictors. All analyses were completed using Python v3.8.5 and SPSS v24.

REFERENCES

- 575 1. Al-Zaiti S, Macleod MR, Van Dam PM, Smith SW, Birnbaum Y. Emerging ECG Methods for
576 Acute Coronary Syndrome Detection: Recommendations & Future Opportunities. *Journal of*
577 *Electrocardiology*. 2022;74:65-72.
- 578 2. Birnbaum Y, Wilson JM, Fiol M, de Luna AB, Eskola M, Nikus K. ECG diagnosis and
579 classification of acute coronary syndromes. *Annals of Noninvasive Electrocardiology*.
580 2014;19(1):4-14.
- 581 3. Goodacre S, Pett P, Arnold J, et al. Clinical diagnosis of acute coronary syndrome in patients
582 with chest pain and a normal or non-diagnostic electrocardiogram. *Emergency medicine journal*.
583 2009;26(12):866-870.
- 584 4. Ioannidis JP, Salem D, Chew PW, Lau J. Accuracy and clinical effect of out-of-hospital
585 electrocardiography in the diagnosis of acute cardiac ischemia: a meta-analysis. *Annals of*
586 *emergency medicine*. 2001;37(5):461-470.
- 587 5. Thygesen K, Alpert JS, Jaffe AS, et al. Fourth universal definition of myocardial infarction
588 (2018). *European Heart Journal*. 2018:ehy462-ehy462.
- 589 6. Gulati M, Levy PD, Mukherjee D, et al. 2021 AHA/ACC/ASE/CHEST/SAEM/SCCT/SCMR
590 Guideline for the Evaluation and Diagnosis of Chest Pain. *Journal of the American College of*
591 *Cardiology*. 2021;78(22):e187-e285.
- 592 7. Levine GN, Bates ER, Blankenship JC, et al. 2015 ACC/AHA/SCAI focused update on primary
593 percutaneous coronary intervention for patients with ST-elevation myocardial infarction: an
594 update of the 2011 ACCF/AHA/SCAI guideline for percutaneous coronary intervention and the
595 2013 ACCF/AHA guideline for the management of ST-elevation myocardial infarction. *Journal of*
596 *the American College of Cardiology*. 2016;67(10):1235-1250.

Formatted: Font: (Default) Arial

597 8. Amsterdam EA, Wenger NK, Brindis RG, et al. 2014 AHA/ACC Guideline for the Management
598 of Patients With Non–ST-Elevation Acute Coronary Syndromes: Executive Summary.
599 *Circulation*. 2014;130(25):2354-2394.

600 9. Dixon WC, Wang TY, Dai D, et al. Anatomic distribution of the culprit lesion in patients with
601 non–ST-segment elevation myocardial infarction undergoing percutaneous coronary
602 intervention: findings from the National Cardiovascular Data Registry. *Journal of the American
603 College of Cardiology*. 2008;52(16):1347-1348.

604 10. Wang TY, McCoy LA, Bhatt DL, et al. Multivessel vs culprit-only percutaneous coronary
605 intervention among patients 65 years or older with acute myocardial infarction. *American heart
606 journal*. 2016;172:9-18.

607 11. Karwowski J, Gierlotka M, Gašior M, et al. Relationship between infarct artery location, acute
608 total coronary occlusion, and mortality in STEMI and NSTEMI patients. *Polish Archives of
609 Internal Medicine*. 2017;127(6):401-411.

610 12. Figueras J, Otaegui I, Marti G, et al. Area at risk and collateral circulation in a first acute
611 myocardial infarction with occluded culprit artery. STEMI vs non-STEMI patients. *International
612 Journal of Cardiology*. 2018;259:14-19.

613 13. Tanaka T, Miki K, Akahori H, et al. Comparison of coronary atherosclerotic disease burden
614 between ST-elevation myocardial infarction and non-ST-elevation myocardial infarction: Non-
615 culprit Gensini score and non-culprit SYNTAX score. *Clinical Cardiology*. 2021;44(2):238-243.

616 14. Aslanger EK, Meyers HP, Bracey A, Smith SW. The STEMI/NonSTEMI Dichotomy needs to be
617 replaced by Occlusion MI vs. Non-Occlusion MI. *International Journal of Cardiology*.
618 2021;330:15.

Formatted: Font: (Default) Cambria Math

Formatted: Font: (Default) Arial

Formatted: Font: (Default) Cambria Math

Formatted: Font: (Default) Arial

Formatted: Font: (Default) Cambria Math

Formatted: Font: (Default) Arial

Formatted: Font: (Default) Cambria Math

Formatted: Font: (Default) Arial

Formatted: Font: (Default) Cambria Math

Formatted: Font: (Default) Arial

- 619 15. Avdikos G, Michas G, Smith SW. From Q/Non-Q Myocardial Infarction to STEMI/NSTEMI: Why
620 It's Time to Consider Another Simplified Dichotomy; a Narrative Literature Review. *Archives of*
621 *Academic Emergency Medicine*. 2022;10(1):e78-e78.
- 622 16. Aslanger EK, Meyers PH, Smith SW. STEMI: A transitional fossil in MI classification? *Journal of*
623 *Electrocardiology*. 2021;65:163-169.
- 624 17. Meyers HP, Bracey A, Lee D, et al. Comparison of the ST-elevation myocardial infarction
625 (STEMI) vs. NSTEMI and occlusion MI (OMI) vs. NOMI paradigms of acute MI. *The Journal of*
626 *emergency medicine*. 2021;60(3):273-284.
- 627 18. Bouzid Z, Faramand Z, Gregg RE, et al. In search of an optimal subset of ECG features to
628 augment the diagnosis of acute coronary syndrome at the emergency department. *Journal of*
629 *the American Heart Association*. 2021;10(3):e017871.
- 630 19. Meyers HP, Bracey A, Lee D, et al. Ischemic ST_a Segment Depression Maximal in V1–V4
631 (Versus V5–V6) of Any Amplitude Is Specific for Occlusion Myocardial Infarction (Versus
632 Nonocclusive Ischemia). *Journal of the American Heart Association*. 2021;10(23):e022866.
- 633 20. Birnbaum Y, de Luna AB, Fiol M, et al. Common pitfalls in the interpretation of
634 electrocardiograms from patients with acute coronary syndromes with narrow QRS: a
635 consensus report. *Journal of Electrocardiology*. 2012;45(5):463-475.
- 636 21. Meyers HP, Bracey A, Lee D, et al. Accuracy of OMI ECG findings versus STEMI criteria for
637 diagnosis of acute coronary occlusion myocardial infarction. *IJC Heart & Vasculature*.
638 2021;33:100767.
- 639 22. Al-Zaiti S, Callaway CW, Kozik TM, Carey M, Pelter M. Clinical Utility of Ventricular
640 Repolarization Dispersion for Real-Time Detection of Non-ST Elevation Myocardial Infarction in
641 Emergency Departments. *Journal of the American Heart Association*. 2015;4(7):e002057.

Formatted: Font: (Default) Cambria Math

Formatted: Font: (Default) Arial

- 642 23. Al-Zaiti S, Alrawashdeh M, Martin-Gill C, Callaway C, Mortara D, Nemeč J. Evaluation of Beat-
643 to-Beat Ventricular Repolarization Lability from Standard 12-Lead ECG During Acute Myocardial
644 Ischemia. *Journal of Electrocardiology*. 2017;50(6):717-724.
- 645 24. Al-Zaiti S, Sejdic E, Nemeč J, Callaway C, Soman P, Lux RL. Spatial Indices of Repolarization
646 Correlate with Non-ST Elevation Myocardial Ischemia in Patients with Chest Pain. *Medical &*
647 *Biological Engineering & Computing* 2018;56(1):1-12.
- 648 25. Sharma A, Miranda DF, Rodin H, Bart BA, Smith SW, Shroff GR. Interobserver variability
649 among experienced electrocardiogram readers to diagnose acute thrombotic coronary occlusion
650 in patients with out of hospital cardiac arrest: Impact of metabolic milieu and angiographic
651 culprit. *Resuscitation*. 2022;172:24-31.
- 652 26. Gregg RE, Yang T, Smith SW, Babaeizadeh S. ECG reading differences demonstrated on two
653 databases. *Journal of Electrocardiology*. 2021;69:75-78.
- 654 27. Cook DA, Oh S-Y, Pusic MV. Accuracy of physicians' electrocardiogram interpretations: a
655 systematic review and meta-analysis. *JAMA internal medicine*. 2020;180(11):1461-1471.
- 656 28. McRae AD, Innes G, Graham M, et al. Undetectable concentrations of an FDA-approved high-
657 sensitivity cardiac Troponin T assay to rule out acute myocardial infarction at emergency
658 department arrival. *Academic Emergency Medicine*. 2017;24:DOI: 10.1111/acem.13229.
- 659 29. Body R, Mahler S. Welcome to the real world: Do the conditions of FDA approval devalue high
660 sensitivity troponin? *Academic Emergency Medicine*. 2017;24:DOI: 10.1111/acem.13256.
- 661 30. Wereski R, Chapman AR, Lee KK, et al. High-sensitivity cardiac troponin concentrations at
662 presentation in patients with ST-segment elevation myocardial infarction. *JAMA cardiology*.
663 2020;5(11):1302-1304.

Formatted: Font: (Default) Cambria Math

Formatted: Font: (Default) Arial

Formatted: Font: (Default) Cambria Math

Formatted: Font: (Default) Arial

- 664 31. Cotterill PG, Deb P, Shrank WH, Pines JM. Variation in chest pain emergency department
665 admission rates and acute myocardial infarction and death within 30 days in the Medicare
666 population. *Academic Emergency Medicine*. 2015;22(8):955-964.
- 667 32. Kang MG, Kang Y, Kim K, et al. Cardiac mortality benefit of direct admission to percutaneous
668 coronary intervention-capable hospital in acute myocardial infarction: Community registry-based
669 study. *Medicine (Baltimore)*. 2021;100(10):e25058-e25058.
- 670 33. Quinn T, Johnsen S, Gale CP, et al. Effects of prehospital 12-lead ECG on processes of care
671 and mortality in acute coronary syndrome: a linked cohort study from the Myocardial Ischaemia
672 National Audit Project. *Heart*. 2014;100(12):944-950.
- 673 34. Bouzid Z, Faramand Z, Martin-Gill C, et al. Incorporation of Serial 12-Lead Electrocardiogram
674 With Machine Learning to Augment the Out-of-Hospital Diagnosis of Non-ST Elevation Acute
675 Coronary Syndrome. *Annals of Emergency Medicine*. 2023;81(1):57-69.
- 676 35. Al-Zaiti S, Besomi L, Bouzid Z, et al. Machine learning-based prediction of acute coronary
677 syndrome using only the pre-hospital 12-lead electrocardiogram. *Nature communications*.
678 2020;11(3966):<https://doi.org/10.1038/s41467-41020-17804-41462>.
- 679 36. Stopyra JP, Harper WS, Higgins TJ, et al. Prehospital modified HEART score predictive of 30-
680 day adverse cardiac events. *Prehospital and disaster medicine*. 2018;33(1):58-62.
- 681 37. Ashburn NP, Snively AC, O'Neill JC, et al. Performance of the European Society of Cardiology
682 0/1-Hour Algorithm With High-Sensitivity Cardiac Troponin T Among Patients With Known
683 Coronary Artery Disease. *JAMA Cardiology*. 2023.
- 684 38. Sabatine MS, Morrow DA, McCabe CH, Antman EM, Gibson CM, Cannon CP. Combination of
685 quantitative ST deviation and troponin elevation provides independent prognostic and
686 therapeutic information in unstable angina and non-ST-elevation myocardial infarction.
687 *American heart journal*. 2006;151(1):25-31.

Formatted: Font: (Default) Arial

Formatted: Font: (Default) Arial

- 688 39. Lux RL. Non-ST-Segment Elevation Myocardial Infarction: A Novel and Robust Approach for
689 Early Detection of Patients at Risk. *Journal of the American Heart Association*.
690 2015;4(7):e002279.
- 691 40. Marrusa S, Zhangc M, Arthurb M. Identification of Acute Coronary Syndrome via Activation and
692 Recovery Times in Body-Surface Mapping and Inverse Electrocardiography. *International*
693 *Journal of Bioelectromagnetism*. 2019;21(1-6).
- 694 41. Lux RL. Basis and ECG measurement of global ventricular repolarization. *Journal of*
695 *Electrocardiology*. 2017;50(6):792-797.
- 696 42. Al-Zaiti S, Runco K, Carey M. Increased T-Wave Complexity Can Indicate Subclinical
697 Myocardial Ischemia in Asymptomatic Adults. *Journal of Electrocardiology*. 2011;44(6):684-688.
- 698 43. Forberg JL, Green M, Björk J, et al. In search of the best method to predict acute coronary
699 syndrome using only the electrocardiogram from the emergency department. *Journal of*
700 *Electrocardiology*. 2009;42:58-63.
- 701 44. Green M, Bjork J, Forberg J, Ekelund U, Edenbrandt L, Ohlsson M. Comparison between neural
702 networks and multiple logistic regression to predict acute coronary syndrome in the emergency
703 room. *Artificial Intelligence in Medicine*. 2006;38:305-318.
- 704 45. Hong S, Zhou Y, Shang J, Xiao C, Sun J. Opportunities and challenges of deep learning
705 methods for electrocardiogram data: A systematic review. *Computers in Biology and Medicine*.
706 2020;122:103801.
- 707 46. Baxt WG, Skora J. Prospective validation of artificial neural network trained to identify acute
708 myocardial infarction. *The Lancet*. 1996;347(8993):12-15.
- 709 47. Tsien CL, Fraser HS, Long WJ, Kennedy RL. Using classification tree and logistic regression
710 methods to diagnose myocardial infarction. *Studies in health technology and informatics*.
711 1998;52 Pt 1:493-497.

Formatted: Font: (Default) Cambria Math

Formatted: Font: (Default) Arial

Formatted: Font: (Default) Cambria Math

Formatted: Font: (Default) Arial

- 712 48. Berikol GB, Yildiz O, Özcan İT. Diagnosis of Acute Coronary Syndrome with a Support Vector
713 Machine. *Journal of Medical Systems*. 2016;40(84).
- 714 49. Wu C-C, Hsu W-D, Islam M, et al. An artificial intelligence approach to early predict non-ST-
715 elevation myocardial infarction patients with chest pain. *Computer Methods and Programs in*
716 *Biomedicine*. 2019;173:109-117.
- 717 50. Brisk R, Bond R, Finlay D, et al. Neural networks for ischaemia detection: Revolution or red
718 herring? A systematic review and meta-analysis. *Journal of Electrocardiology*. 2021;69:79.
- 719 51. Bond R, Finlay D, Al-Zaiti SS, Macfarlane P. Machine learning with electrocardiograms: A call
720 for guidelines and best practices for 'stress testing' algorithms. *Journal of Electrocardiology*.
721 2021;69S:1-6.
- 722 52. Elul Y, Rosenberg AA, Schuster A, Bronstein AM, Yaniv Y. Meeting the unmet needs of
723 clinicians from AI systems showcased for cardiology with deep-learning-based ECG analysis.
724 *Proceedings of the National Academy of Sciences*. 2021;118(24):e2020620118.
- 725 53. Cohen MV, Downey JM. What are optimal P2Y12 inhibitor and schedule of administration in
726 patients with acute coronary syndrome? *Journal of Cardiovascular Pharmacology and*
727 *Therapeutics*. 2020;25(2):121-130.
- 728 54. Tziakas D, Chalikias G, Al-Lamee R, Kaski JC. Total coronary occlusion in non ST elevation
729 myocardial infarction: Time to change our practice? *International Journal of Cardiology*.
730 2021;329:1-8.
- 731 55. Udelson JE, Selker HP, Braunwald E. Glucose-Insulin-Potassium Therapy for Acute
732 Myocardial Infarction: 50 Years On and Time for a Relook. *Circulation*. 2022;146(7):503-505.
- 733 56. Zvuloni E, Read J, Ribeiro AH, Ribeiro ALP, Behar JA. On Merging Feature Engineering and
734 Deep Learning for Diagnosis, Risk-Prediction and Age Estimation Based on the 12-Lead ECG.
735 *arXiv preprint arXiv:220706096*. 2022.

- 736 57. Al-Zaiti SS, Martin-Gill C, Sejdic E, Alrawashdeh M, Callaway C. Rationale, development, and
737 implementation of the Electrocardiographic Methods for the Prehospital Identification of Non-ST
738 Elevation Myocardial Infarction Events (EMPIRE). *J Electrocardiol.* 2015;48(6):921-926.
- 739 58. Zègre-Hemsey JK, Hogg M, Crandell J, et al. Prehospital ECG with ST-depression and T-wave
740 inversion are associated with new onset heart failure in individuals transported by ambulance for
741 suspected acute coronary syndrome. *Journal of Electrocardiology.* 2021.
- 742 59. Al-Zaiti SS, Alghwiri AA, Hu X, et al. A clinician's guide to understanding and critically appraising
743 machine learning studies: a checklist for Ruling Out Bias Using Standard Tools in Machine
744 Learning (ROBUST-ML). *European Heart Journal-Digital Health.* 2022;3(2):125-140.
- 745 60. Al-Zaiti SS, Faramand Z, Alrawashdeh MO, Sereika SM, Martin-Gill C, Callaway C. Comparison
746 of clinical risk scores for triaging high-risk chest pain patients at the emergency department. *The*
747 *American journal of emergency medicine.* 2019;37(3):461-467.

748

749 **Table 1. Baseline demographic and clinical characteristics**

| | DERIVATION & TESTING COHORT (N=4,026) | EXTERNAL VALIDATION COHORT (N=3,287) |
|----------------------------------|------------------------------------------------------|-------------------------------------------------|
| AGE (YEARS) | 59±16 (18–102) | 60±15 (21–100) |
| SEX | | |
| Male | 2,122 (53%) | 1,814 (55%) |
| Female | 1,904 (47%) | 1,473 (45%) |
| RACE | | |
| White | 1,698 (42%) | 1,326 (40%) |
| Black | 1,328 (33%) | 1,544 (47%) |
| Others | 52 (1.3%) | 40 (1%) |
| Unknown | 948 (24%) | 377 (12%) |
| ETHNICITY | | |
| Not Hispanic | 3,043 (76%) | 2,850 (87%) |
| Hispanic / Latino | 19 (1%) | 116 (3.5%) |
| Unknown | 964 (23%) | 321 (9.5%) |
| PAST MEDICAL HISTORY | | |
| Hypertension | 2,767 (69%) | 2,090 (64%) |
| Diabetes | 1,146 (29%) | 1,067 (33%) |
| High cholesterol | 1,520 (38%) | 1,376 (42%) |
| Current smoker | 1,244 (31%) | 802 (25%) |
| Known CAD | 1,388 (35%) | 964 (30%) |
| Prior MI | 930 (23%) | 929 (29%) |
| Prior PCI | 963 (24%) | 134 (4%) |
| Prior CABG | 357 (10%) | 470 (14%) |
| ECG & LAB FINDINGS | | |
| Sinus rhythm | 3,496 (87%) | 2,614 (80%) |
| Atrial fibrillation | 354 (9%) | 352 (11%) |
| Left BBB | 94 (2.3%) | 114 (3.5%) |
| Right BBB | 237 (5.9%) | 215 (6.6%) |
| ECG-LVH | 383 (9.5%) | 467 (14.2%) |
| cTnI positive (initial) | 330 (8.2%) | 736 (22.4%) |
| cTnI positive (serial testing) | 729 (18.1%) | 1,177 (35.8%) |
| MEDICAL THERAPY | | |
| PCI (ANY STENT) | 300 (7.5%) | 245 (7.5%) |
| <i>Emergent PCI (<90 MIN)</i> | 144 (3.6%) | 157 (4.8%) |
| <i>Total LAD occlusion</i> | 91 (2.3%) | 94 (2.9%) |
| <i>Total LCX occlusion</i> | 63 (1.6%) | 88 (2.7%) |
| <i>Total RCA occlusion</i> | 101 (2.5%) | 102 (3.1%) |
| CABG | 34 (0.8%) | 30 (0.9%) |
| STUDY OUTCOMES | | |
| CONFIRMED ACS | 550 (13.7%) | 537 (16.3%) |
| OMI | 210 (5.2%) | 209 (6.4%) |
| <i>Other Acute MI (NOMI)</i> | 240 (6.0%) | 220 (6.7%) |
| <i>Unstable Angina</i> | 100 (2.5%) | 108 (3.3%) |
| 30-DAY CV DEATH | 137 (3.4%) | 111 (3.4%) |

750 Values are mean ± SD (min-max) or n (%); CAD: coronary artery disease; MI: myocardial infarction; BBB: bundle
751 branch block; LVH: left ventricular hypertrophy; PCI: percutaneous coronary intervention; LAD: left anterior
752 descending artery; LCX: left circumflex artery; RCA: right coronary artery; CABG: coronary artery bypass graft;
753 OMI: occlusion MI; NOMI: non-occlusion MI; CV: cardiovascular.

754 **FIGURE LEGENDS**

755 **Fig. 1. Cohort and sample selection**

756 This flow diagram shows patient inclusion and exclusion in each cohort, as well as the dataset partition
757 for training, internal testing, and external validation. Exclusions are not mutually exclusive.

758 **Fig. 2. Algorithm derivation and testing**

759 This figure shows (A) the classification performance of the machine learning model against other
760 reference standards for detecting occlusion myocardial infarction (OMI), (B) the probability density plots
761 of OMI(+) and OMI(-) classes as denoted by the machine learning model, along with optimal cutoffs of
762 low-risk, intermediate, and high-risk, and (C) distribution of patients in low-risk (+), intermediate risk
763 (++) and high-risk (+++) as per the machine learning model and HEART score.

764 **Fig. 3. Model explainability for OMI detection**

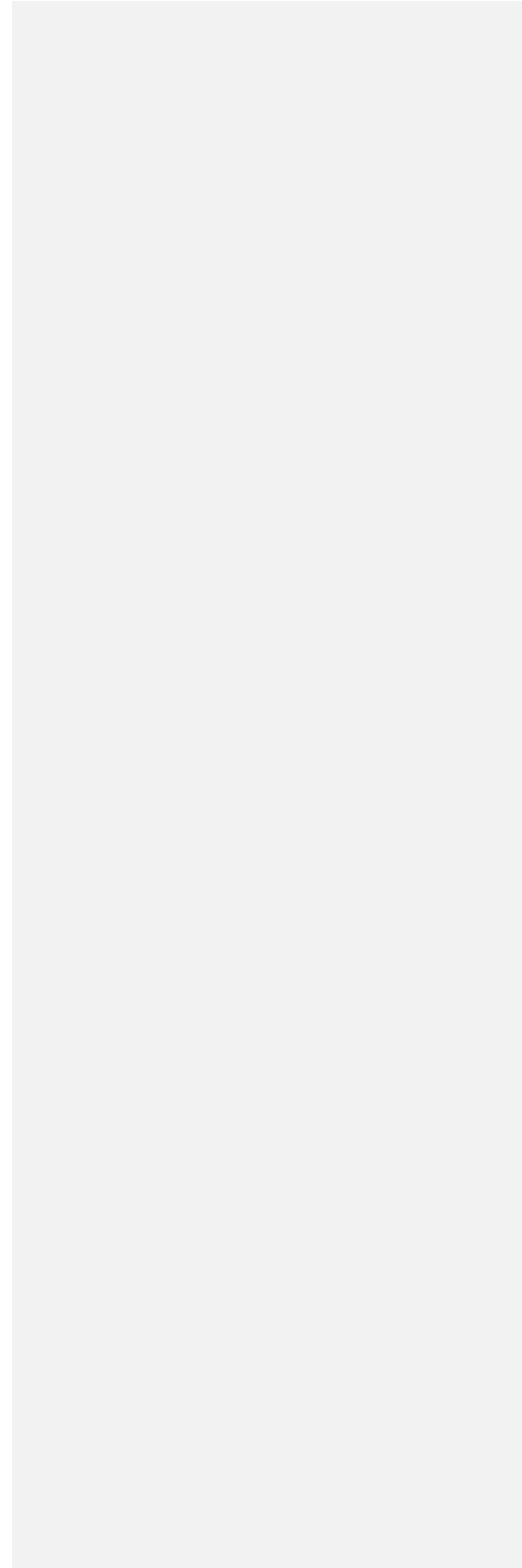
765 This figure shows (A) SHAP values for the 25 most important features driving the predictions of the
766 machine learning classifier in the derivation cohort, and (B) the aggregate median beats of ECGs with
767 occlusion myocardial infarction (OMI) class (red) and the aggregate median beats of ECGs with normal
768 sinus rhythm and no OMI (blue).

769 **Fig. 4. External validation of ECG-SMART algorithm**

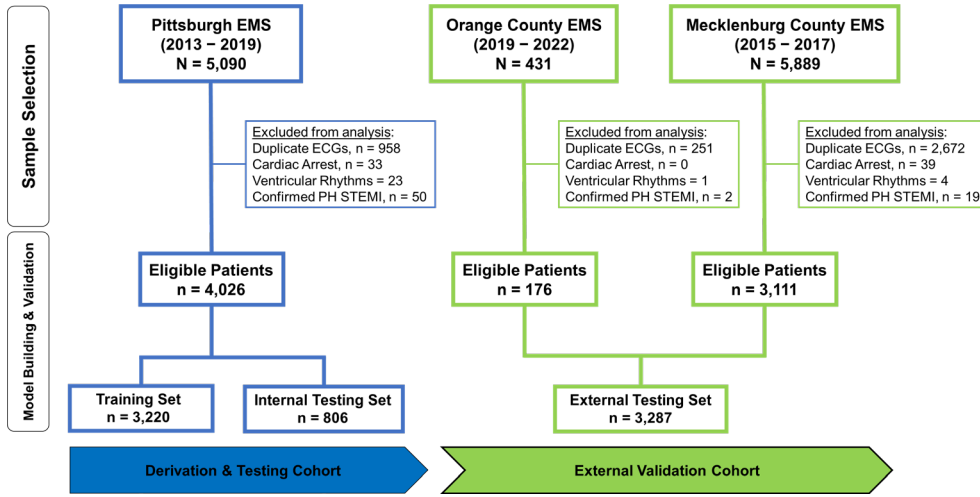
770 This figure shows (A) the classification performance of the machine learning model against other
771 reference standards for detecting occlusion myocardial infarction (OMI), (B) the independent clinical
772 predictors of OMI on multivariate logistic regression testing, and (C) the overall sensitivity and
773 specificity (95% confidence interval [CI]) of the derived OMI score, along with breakdown across
774 subgroups based on age, sex, comorbidities, and baseline ECG findings. The size of markers denotes
775 the sample size of the respective subgroup.

776 **Fig. 5. Net reclassification improvement of OMI risk score when integrated in the clinical**
777 **workflow at first medical contact** **Decision-analysis for the incremental gain of OMI risk score in**
778 **reclassifying patients**

779 This figure simulates the incremental gain of the derived risk score in reclassifying the initial triage
780 decisions by emergency personnel at first medical contact.



781 Fig. 1. Cohort and sample selection

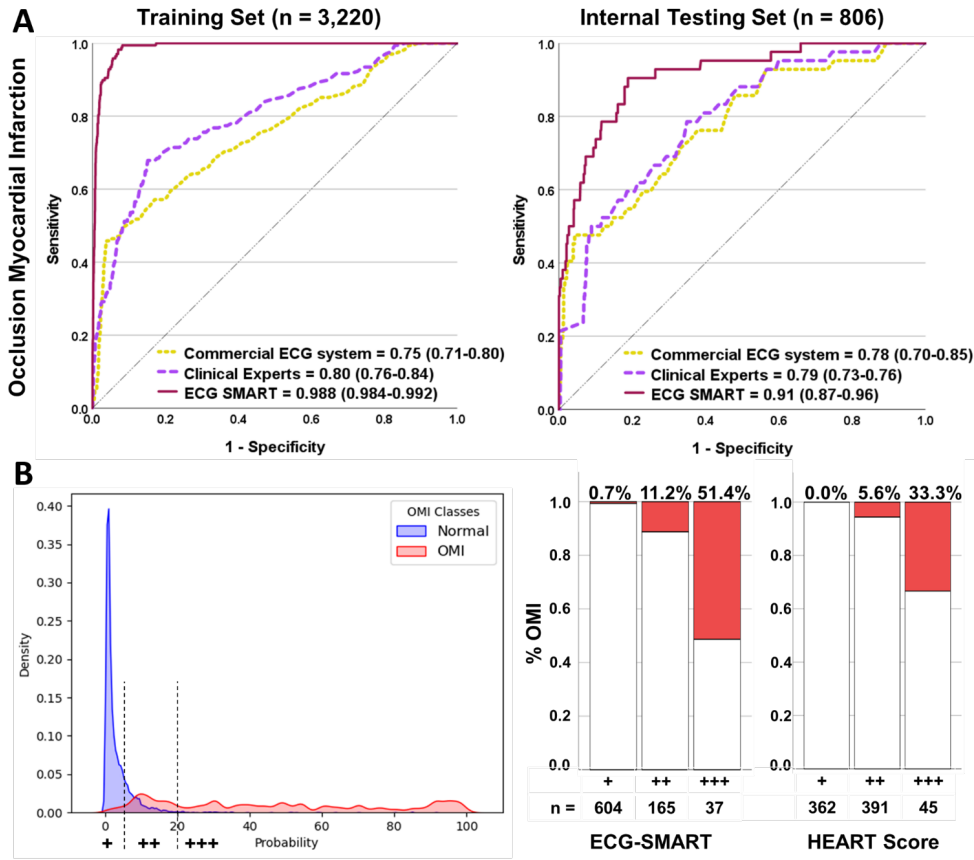


782

783

784

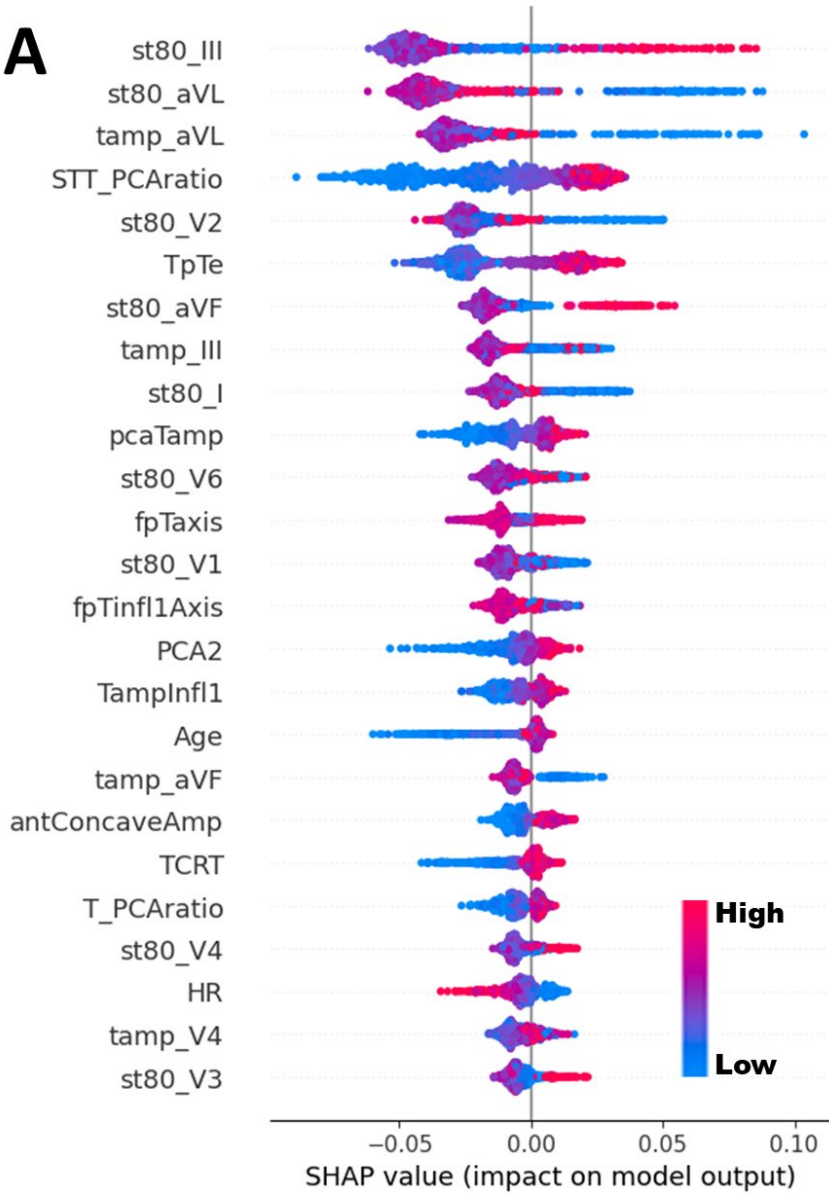
785 **Fig. 2. Algorithm derivation and testing for OMI detection**



786

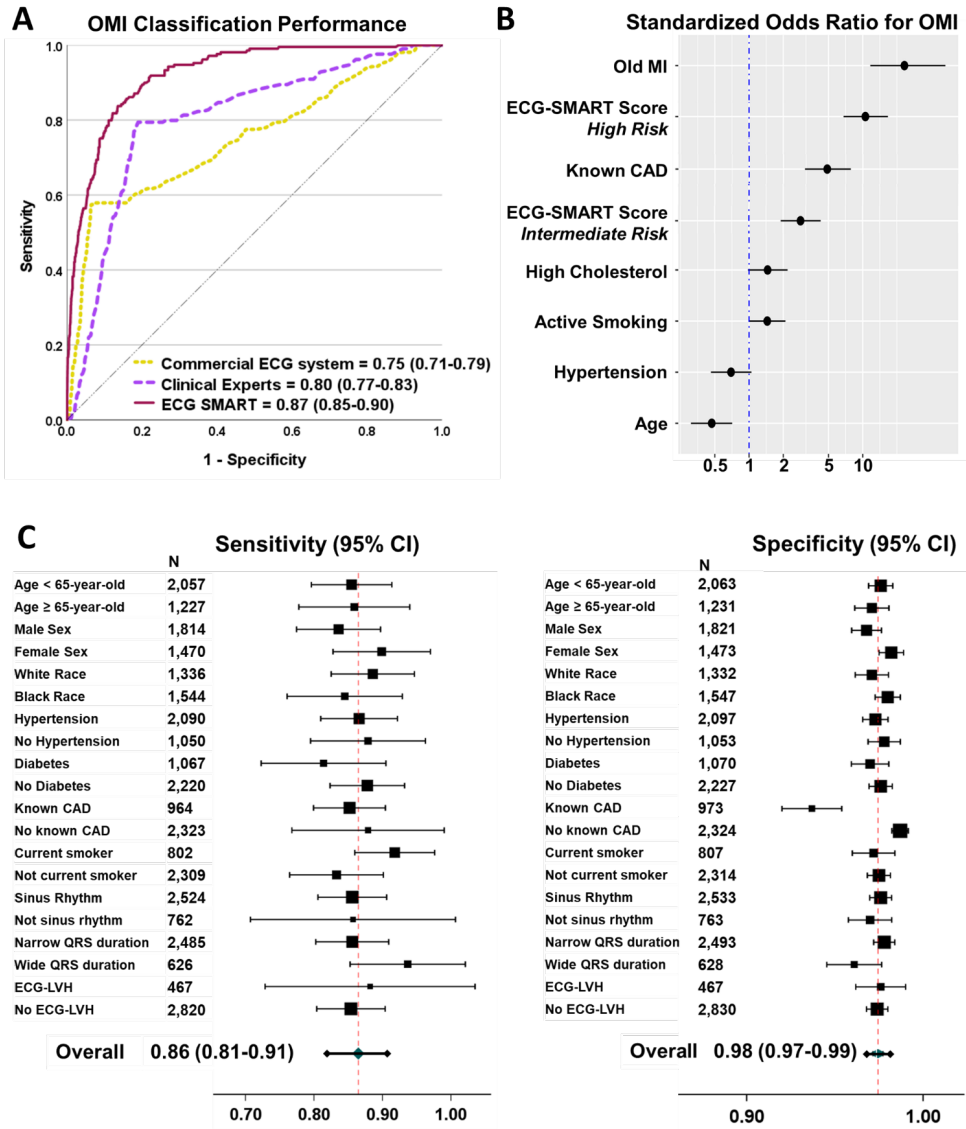
787

A

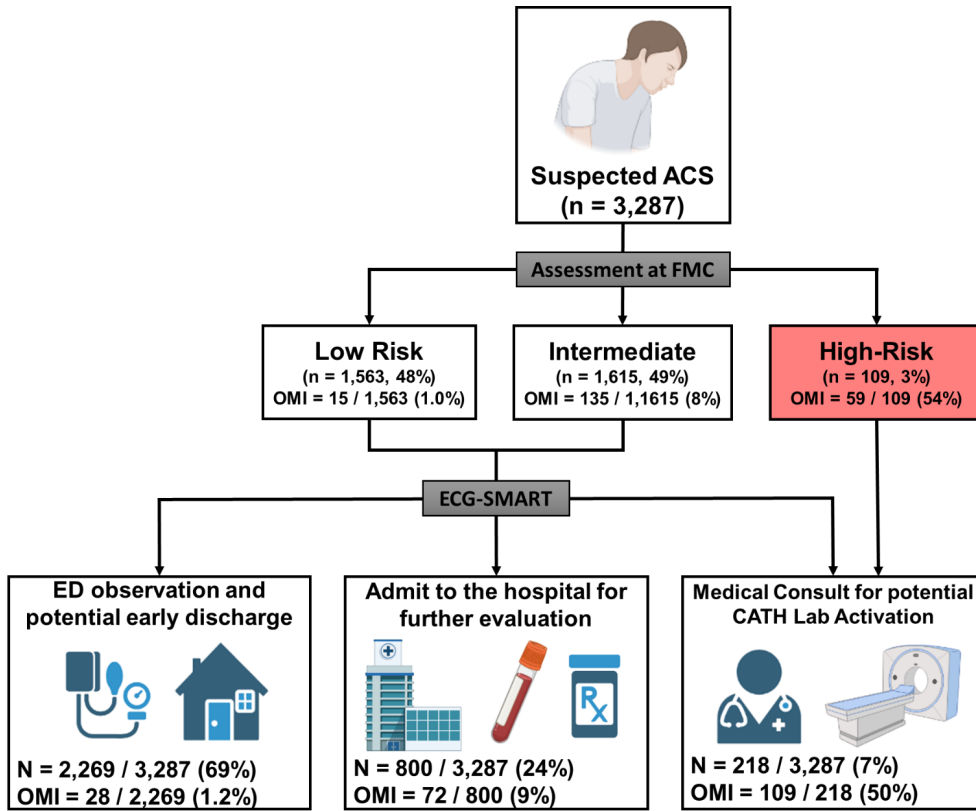




792 Fig. 4. External validation of ECG-SMART algorithm for OMI detection



794 **Fig. 5. Decision analysis for the incremental gain-Net reclassification improvement of OMI risk**
 795 **score when integrated in the clinical workflow re-classifying patients at first medical contact**



796

797

798

DATA SUPPLEMENT

799 Legend for Extended Data Figures

800 **Extended Data Fig. 1. The relationship between the magnitude of vessel occlusion and the** 801 **classification of acute coronary events**

802 This figure shows the spectrum of coronary artery disease (CAD) as a function of severity and extent of
803 atherosclerosis plaque progression, ranging from patent coronary artery (far left) to total coronary
804 occlusion (far right). Among patients who develop symptomatic CAD, including those evaluated for
805 chest pain or angina-like symptoms, a subset is diagnosed with acute coronary syndrome (ACS). This
806 group is subclassified as either acute myocardial infarction (MI) or unstable angina (UA). Those with
807 acute MI can be further subclassified, based on the presence of ST-elevation on the ECG, as either ST-
808 elevation myocardial infarction (STEMI) or without ST-elevation (NSTEMI). The STEMI and NSTEMI
809 patients overlap in terms of the presence or absence of total occlusion (depicted as triangles across the
810 continuum in the figure). Alternatively, the same group with acute MI can be subclassified, based on
811 angiographic TIMI flow criteria, as either occlusion (OMI) or non-occlusion (non-OMI) myocardial
812 infarction. Unlike STEMI, OMI classification better aligns with focal angiographic findings since this
813 group exclusively contains patients with total coronary occlusion. The color gradient indicates the
814 severity of disease. This Figure was created with BioRender.com. Reproduced with permission from Al-
815 Zaiti et. al.¹ (permission number 5471421247333, Licensed content publisher: Elsevier).

816 **Extended Data Fig. 2. Graphical abstract summarizing the flow of study and main findings**

817 This figure provides a graphical summary of the study flow and main findings.

818 **Extended Data Fig. 3. Local explainability of feature importance on a selected example**

819 This figure shows the baseline ECG of a 50-year-old female with a past medical history of
820 hypertension, high cholesterol, prior myocardial infarction, and current smoking. The ECG was
821 documented as benign with isolated non-specific T wave changes, and the patient was triaged as

822 ~~intermediate risk. The OMI score was 62 indicating the need to up triage. The patient was later sent to~~
823 ~~the catheterization lab where she had complete occlusion of the right coronary artery. The OMI score~~
824 ~~on this baseline ECG was 62 indicating high risk designation. The force plot identified the five most~~
825 ~~important ECG features that met the contribution threshold of the random forest model: negative T~~
826 ~~wave in aVL, slight ST depression in aVL and V2, and slight ST elevation in aVF and III.~~

827 **Extended Data Fig. 34. Selected examples of a patients correctly reclassified as OMI**

828 This figure shows ~~two examples of an ECG that was patients who were~~ correctly reclassified as
829 occlusion myocardial infarction by the machine learning model. ~~(A) This Baseline-baseline ECG was for~~
830 ~~of a 67-year-old male with a past medical history of high cholesterol and a prior myocardial~~

831 The ST-depression in anterior-lateral leads were noted, and the patient was triaged as intermediate
832 risk. The OMI score was 49 indicating the need to up-triage. The patient was later sent to the

833 catheterization lab where he had complete occlusion of the right coronary artery. ~~(B) Baseline ECG of a~~
834 ~~50-year-old female with a past medical history of hypertension, high cholesterol, prior myocardial~~
835 ~~infarction, and current smoking. The ECG was documented as benign with isolated non-specific T wave~~
836 ~~changes, and the patient was triaged as intermediate risk. The OMI score was 62 indicating the need to~~
837 ~~up triage. The patient was later sent to the catheterization lab where she had complete occlusion of the~~
838 ~~right coronary artery.~~

839 **Extended Data Fig. 45. Selected example of a missed OMI by our model**

840 This figure provides a selected example of a patient with occlusion myocardial infarction that was
841 missed by the machine learning model and other reference standards. This ECG was obtained on a 70-
842 year-old female with a past medical history of hypertension, high cholesterol, prior myocardial
843 infarction, and current smoking. The baseline clinical interpretation suggests normal sinus rhythm with
844 benign findings. There are isolated Q waves in inferior leads, low ECG voltage, and some baseline
845 wander and high frequency noise in few leads. The OMI risk score was 2 indicating a low risk. The
846 patient was later sent to the catheterization lab, which showed significant left main occlusion and had

847 many stents placed. The patient developed new-onset HF during hospitalization. A closer look at this
848 ECG by experienced ECG readers suggests that this ECG could resemble the “precordial swirl
849 pattern”, a rightward ST-elevation vector, with STE in V1 and aVR and reciprocal ST-depression in V5
850 and V6. This pattern was found to correlate with LAD occlusion.

851 **Extended Data Fig. 56. Development and validation of an algorithm to screen for any ACS event**

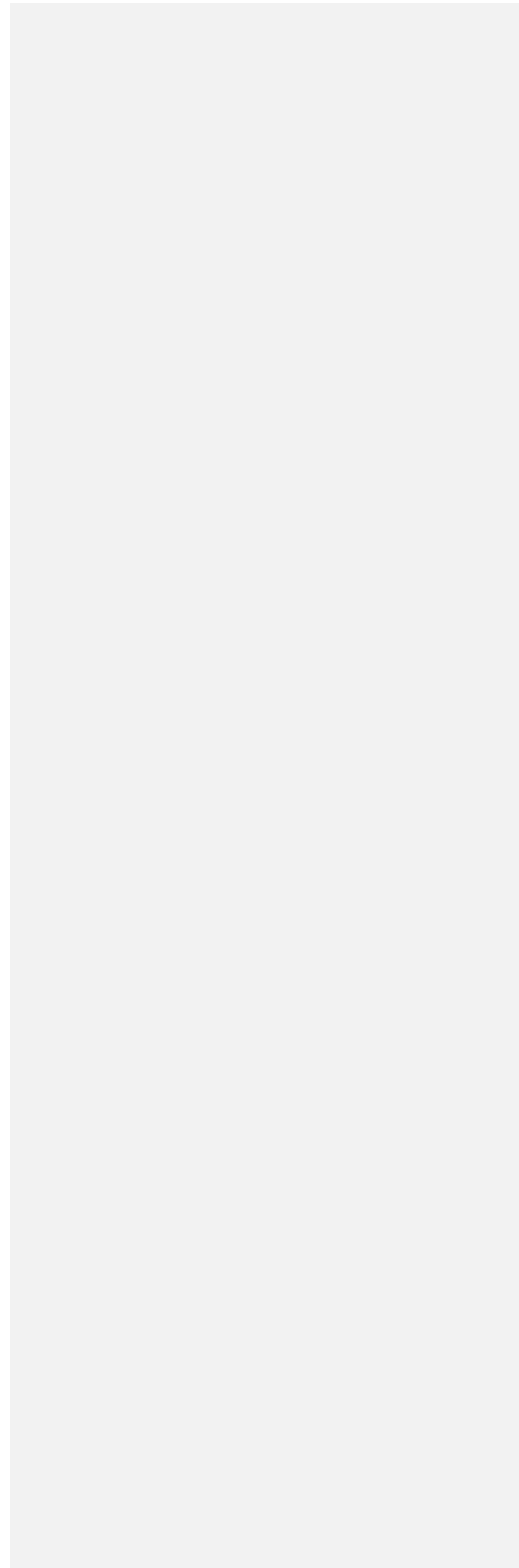
852 This figure shows the classification performance of the machine learning model against other reference
853 standards for detecting any acute coronary syndrome event (ACS). The figure also shows the
854 distribution of patients in low-risk, intermediate risk, and high-risk groups as per our derived risk score.
855 There is a notable gain in precision (rule-in) but a significant loss in recall (rule-out).

856 **Extended Data Fig. 67. Limitations of ST amplitude on surface ECG as a sole marker of**
857 **myocardial ischemia**

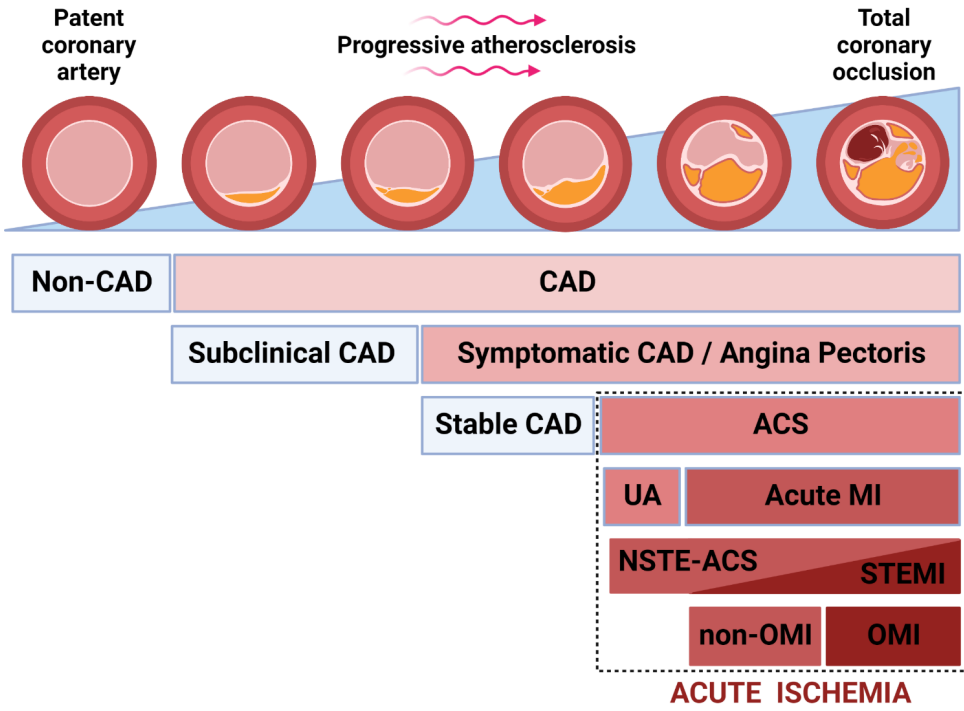
858 This figure shows: (A) cardiac model of anterior wall epicardial ischemia with corresponding ST-
859 elevation on V3 to V5 of the 12-lead ECG. (B) cardiac model of anterolateral and inferior-apical
860 epicardial ischemia with corresponding attenuation of ST changes on the 12-lead ECG. This figure was
861 generated using ECGSIM (www.ecgsim.org). Reproduced with permission from Al-Zaiti et. al.¹
862 (permission number 5471421247333, Licensed content publisher: Elsevier).

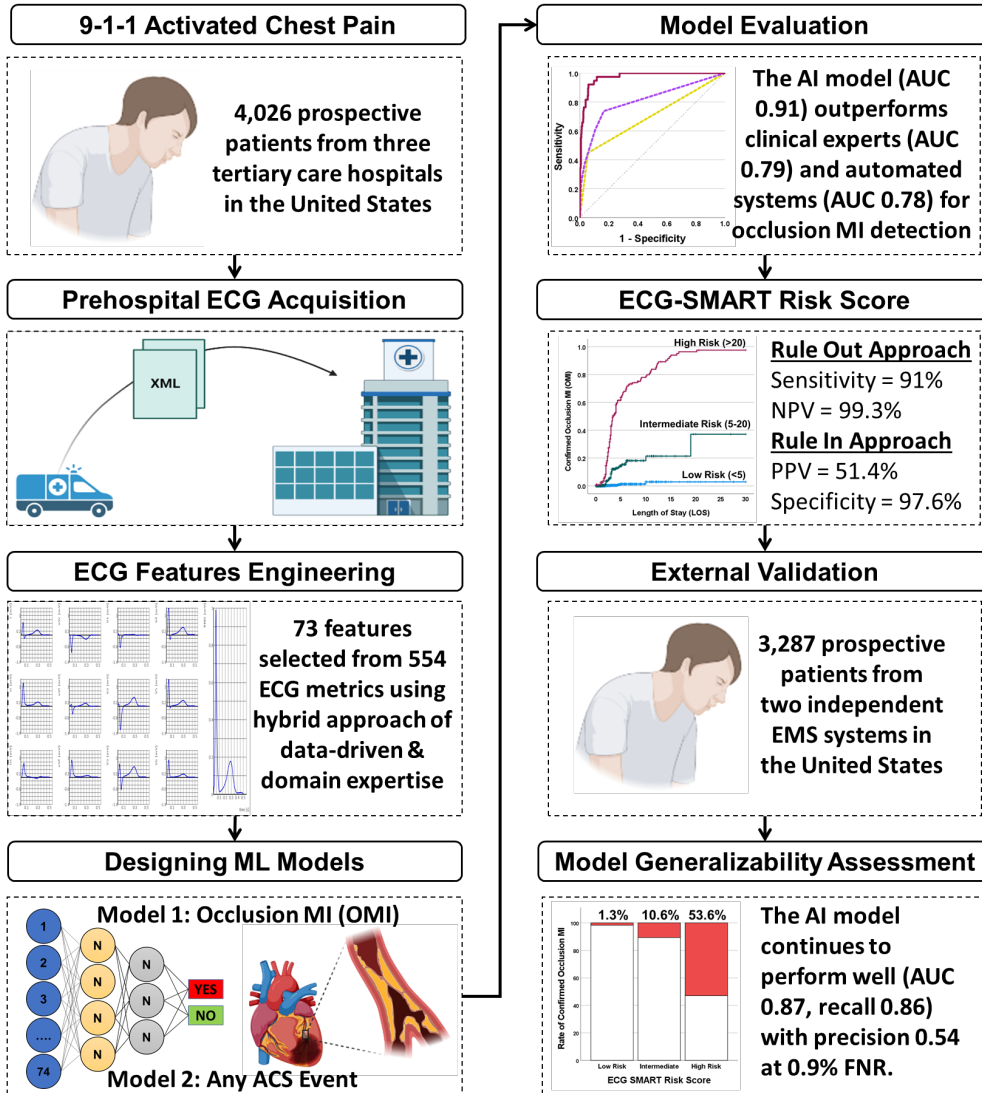
863 **Extended Data Fig. 78. Comparison between 10 algorithms trained on the derivation cohort to**
864 **classify OMI**

865 This figure compares the area under the receiver operator characteristics curves (95% confidence
866 interval) of 10 classifiers during training (left) and testing (right) on the derivation cohort. RF: random
867 forest; KNN: K-nearest neighbors; GBM: gradient boosting machine; XGB: extreme gradient boosting;
868 SVM: support vector machine; ANN: artificial neural networks; LogReg: regularized logistic regression;
869 LDA: linear discriminant analysis; SGD_LogReg: stochastic gradient descent logistic regression; G_NB:
870 Gaussian Naïve Bayes.



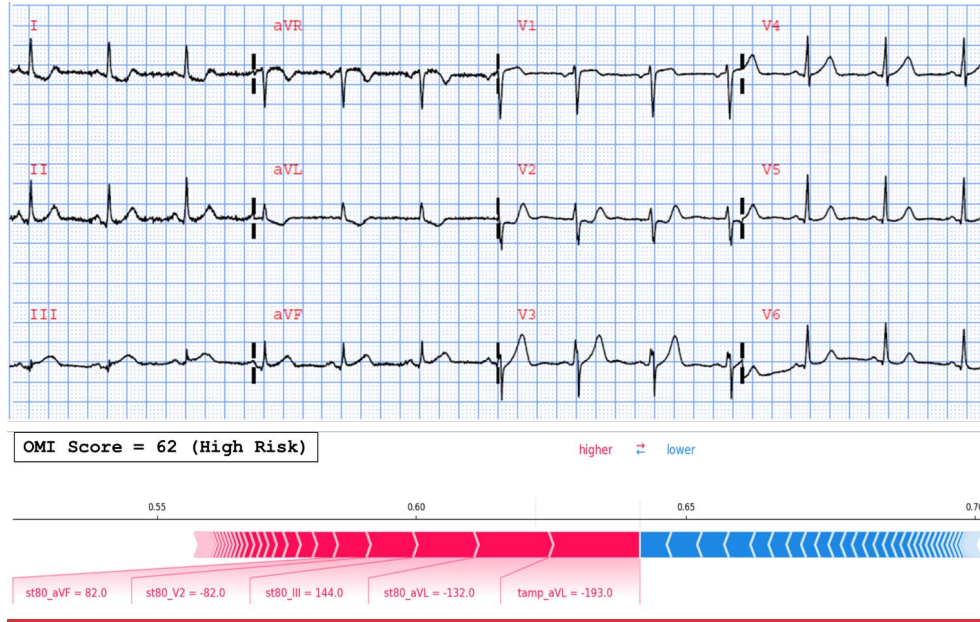
872 **Extended Data Fig 1. The relationship between magnitude of coronary occlusion and coronary**
873 **artery disease and acute events classification**





878

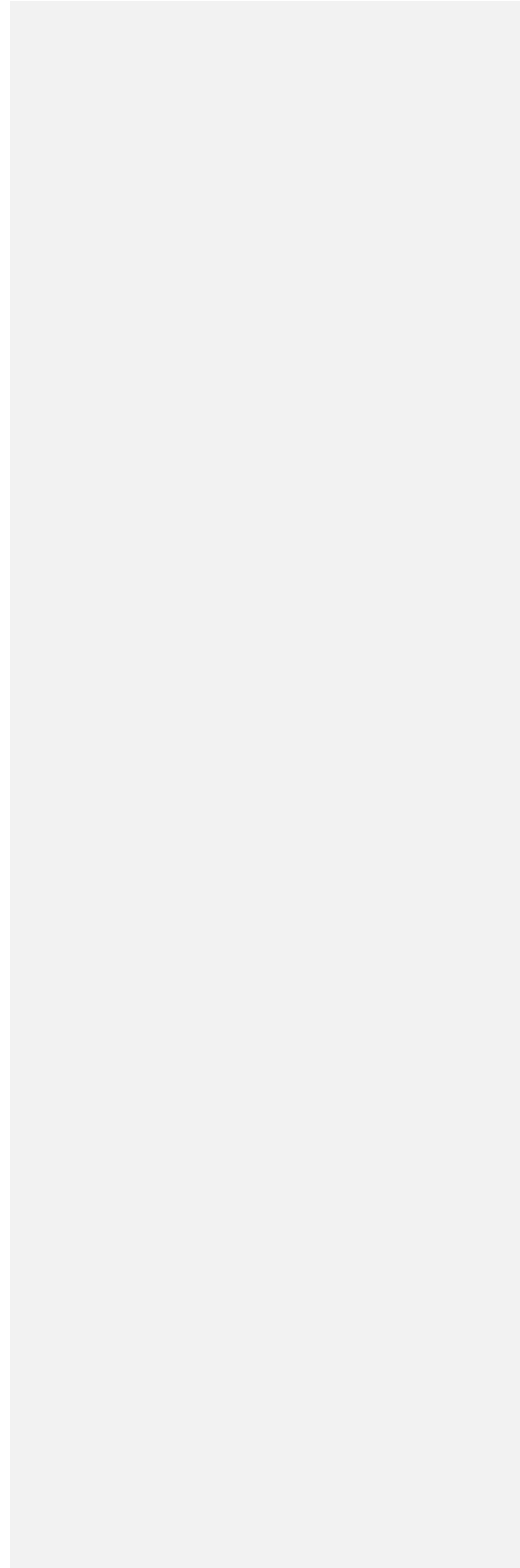
Extended Data Fig. 3. Local explainability of feature importance on a selected example

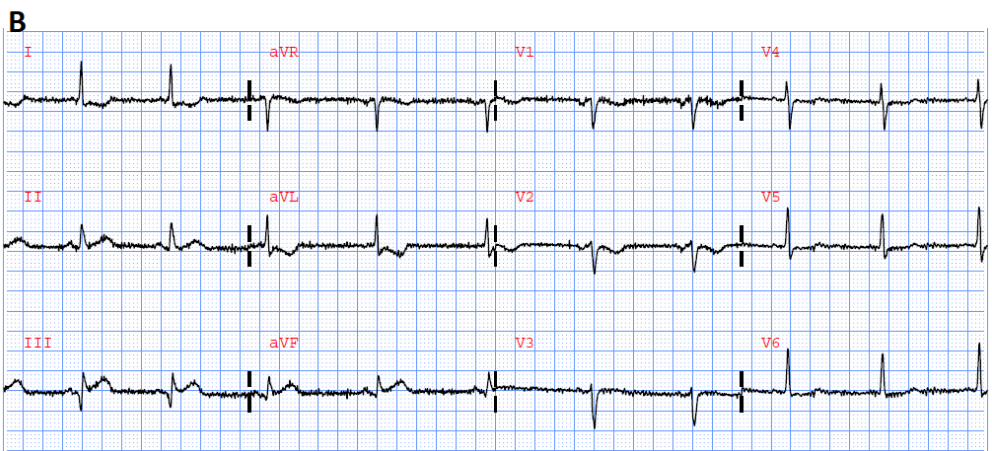
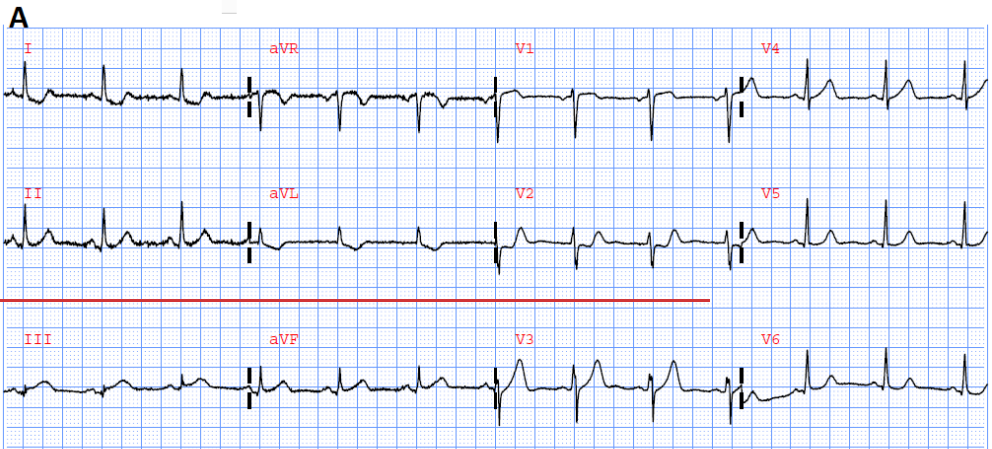


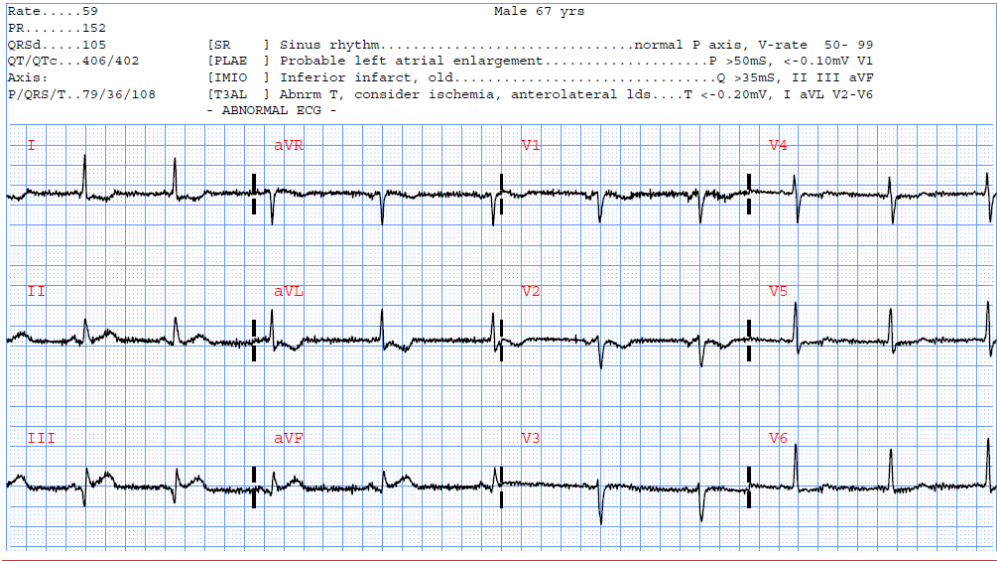
879

880

Extended Data Fig 34. Selected examples of a patients correctly reclassified as OMI





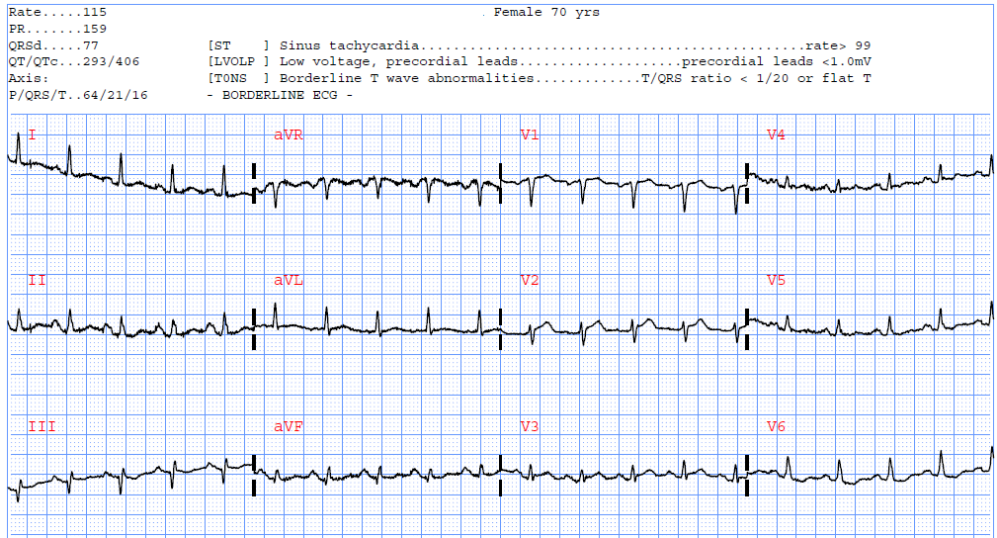


883

884

885

Extended Data Fig 45. Selected example of a missed OMI by our model

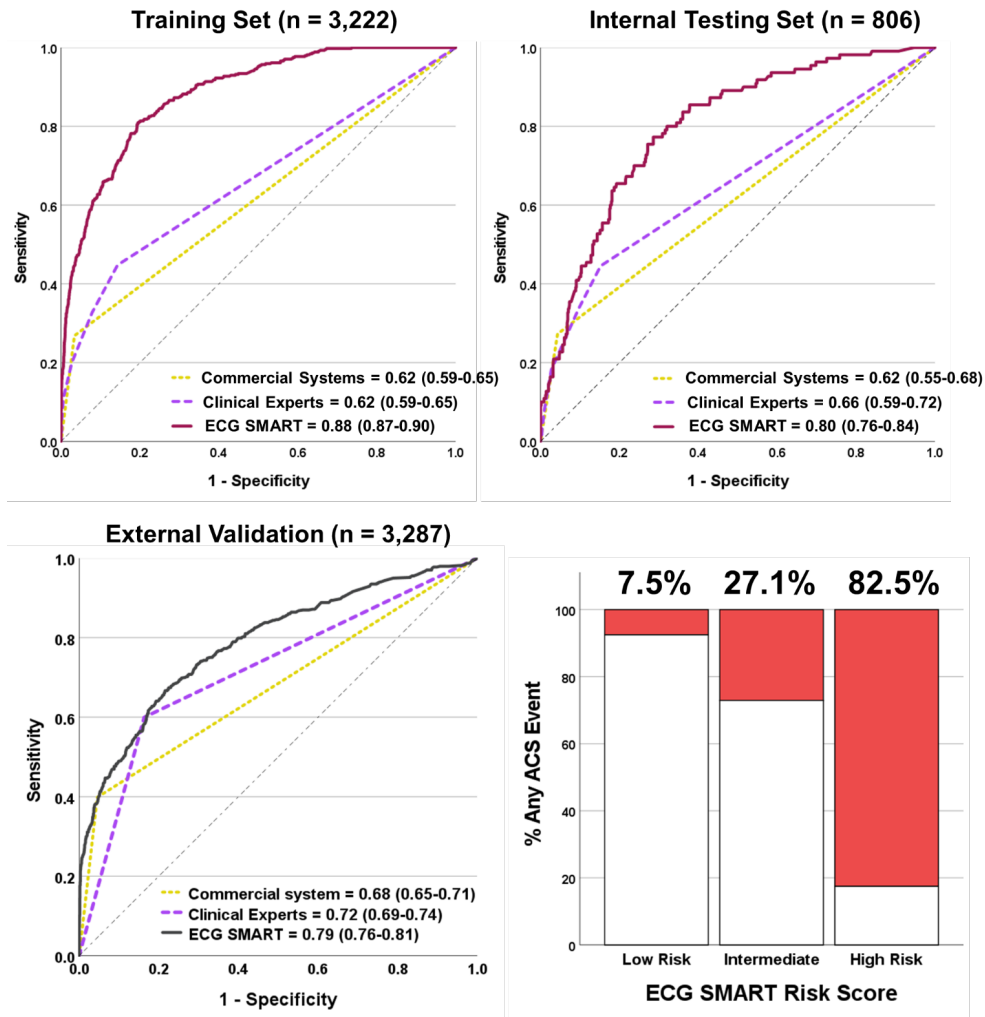


886

887

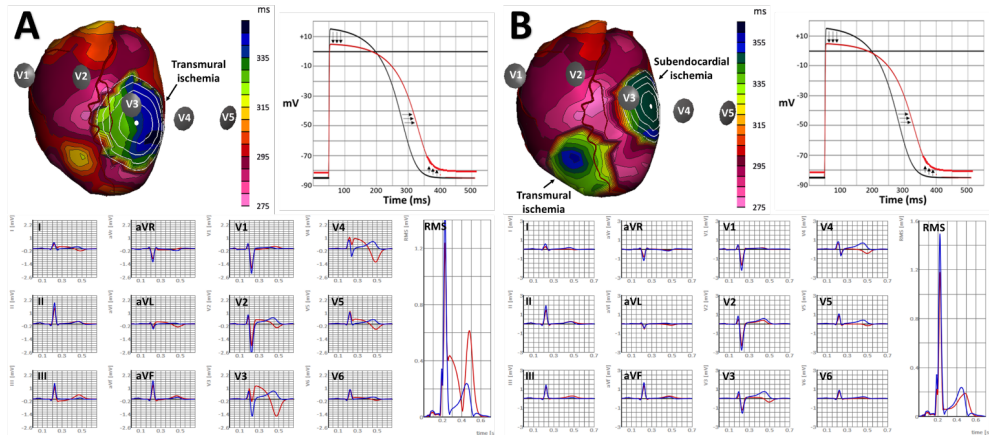
888
889

Extended Data Fig. 56. Development and validation of an algorithm to screen for any ACS event



890
891

892 Extended Data Fig. 67: Limitations of ST amplitude on surface ECG as a sole marker of
893 myocardial ischemia

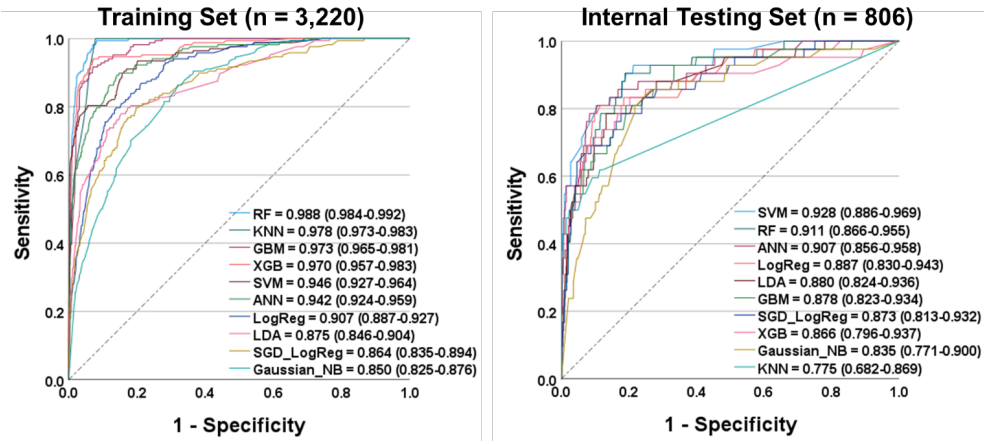


894

895

896

897 **Extended Data Fig 78. Comparison between 10 algorithms trained on the derivation cohort to**
898 **classify OMI**



899